Final report

Recycling of acrylic-based resins from highly aligned short fiber reinforced composite parts

Research stay at
University of Delaware – Center for Composite Materials
from 6 February until 7 July 2023

Dipl.-Ing. Markus Schwaiger BSc.

July 2023

Abstract

This work describes the recycling of an acrylic-based resin reinforced with highly aligned short fiber reinforced composite parts using a pyrolysis process. The feasibility of reclaiming monomer was demonstrated in a step wise optimized small-scale setup by using unreinforced resin and short carbon fiber reinforced composites. By adjusting the depolymerization setup, temperature and time, a monomer content of up to 88% was obtained in the reclaimed resin. Depolymerization by-products were identified using Fourier-transform infrared spectroscopy and were mainly alcohols, various esters or aldehydes. After depolymerization, reclaimed fibers still showed residues on the surfaces and were not dispersible. Short-term oxidation at evaluated temperature under air was proven to make the carbon fibers dispersible, whereas washing with solvents showed no effect on the dispersibility. An addition of 20% crude reclaimed resin (MMA content of 77%) to the neat resin lowered the T_g by 17 °C and the storage modulus at 30 °C by 20%.

Table of content

1 Introduction

Composite materials are made from at least two materials, which differ significantly in physical and/or chemical properties with the aim to improve mechanical performance (fiber reinforcement) or reduce the price (fillers). The most important composites are fiber-reinforced polymers (FRP), which are made from a polymer matrix and a fiber reinforcement (glass, carbon, polymer), resulting in a lightweight material with outstanding specific mechanical properties [1]. This makes them an excellent alternative to conventional materials such as aluminum or steel. For high-performance applications, carbon fiber-reinforced polymers (CFRP) are used in many different applications, including aerospace, automotive and sea vehicles, defense, wind turbines, construction, marine, sports and storage tanks [2].

The increasing demand for high-performance materials in these applications is expected to drive the composite market over the next years. In 2021 the global composite market size was estimated at $88.8 billion and it is expected to increase with an compound annual growth rate of 6.6 % from 2021 to 2028 [3]. The growing market for composites is accompanied by an increase in the amount of waste. There are three major options to deal with composite waste at their end of life: landfill, incineration and recycling [4]. In the EU, there are already four countries (German, Austria, the Netherlands and Finland), which forbid landfilling and incineration of composites [5]. With increasing landfill costs, increasing awareness on circular economy thinking, government policies and legislations [6], the recycling of composites is more relevant than ever.

Currently, there are three common recycling methods, namely mechanical, thermal and chemical recycling. The former is the cheapest method since the composite is only shredded and reused as a filler in applications with lower mechanical requirements. In contrast, in thermal and chemical recycling the polymer is separated from the fiber. Chemical recycling involves the use of chemical solvents to degrade and dissolute the polymer and reclaim the fibers. Since expensive equipment and hazardous solvents are required, this technique is not much used on an industrial scale [7]. Thermal recycling uses high temperatures to decompose the polymer. Herein, pyrolysis is one of the most common thermal recycling techniques. Temperatures in the range of 350 to

700 °C are applied to de-polymerize the polymer into low molecular weight products (gases, liquids) under inert atmosphere [2]. Those low molecular weight products can be used as fuels or resources for other chemical substances [8]. Generally, specific interest is given to the recovery of the carbon fibers since this is the most expensive part of the composite. These reclaimed fibers often require additional treatment to be cleaned from contaminations. However, to account for a higher sustainability, the polymer should be reusable as well. Some polymers like polystyrene, polyamide, polyethylene terephthalate and poly(methyl methacrylate) (PMMA) de-polymerize to their original monomers under pyrolysis [9]. After purification, the monomer can be polymerized again. Thus, by using composites with acrylic-based resins, both the carbon fibers and the resin can be recycled by pyrolysis. This was recently demonstrated in a first proof of concept by recovering both from thermoplastic composites used in marine applications [10]. The reclaimed components (biaxial carbon fabric and methyl methacrylate (MMA) monomer) could be successfully reused to manufacture composites, whereas the differences in mechanical properties were less than 4 % [10].

In contrast to the aforementioned work [10], this project focused on the closed loop recycling of an acrylic-based resin reinforced with TuFF feedstock – a highly aligned discontinuous fiber preform in thin ply-format. The advantage of TuFF feedstocks is that short carbon fibers from recycling and waste stream can also be used without reducing the mechanical properties [11]. Furthermore, by using TuFF feedstocks recycled composite parts are not limited to the size of the recycled carbon fabrics. However, for the production of TuFF preforms from recycled short carbon fibers, the dispersibility of the reclaimed short carbon fibers is crucial [12]. Therefore, it is beneficial when the depolymerization step results in fibers with sufficient quality.

Within this work the feasibility of resin reclamation from unreinforced resin and TuFF composites was demonstrated and the depolymerization process was systematically optimized. The reclaimed monomer (MMA) yield was quantified and by-products were identified. Additionally, reclaimed carbon fibers were analyzed and potential ways for cleaning were explored. Furthermore, the effect of the addition of reclaimed crude resin on the thermo-mechanic properties was investigated.

2 Materials

Within this work Elium 188O resin, supplied by Arkema, Inc. is used. The resin is an acrylic thermoplastic resin and the free-radical polymerization is initiated by a peroxide. As peroxide a pourable benzoyl peroxide paste (Luperox AFR 40) was supplied by Arkema Inc. Based on previous work an amount of 3 wt% Luperox AFR 40 was used [12]. 4-Methoxyphenol (MEHQ) and MMA (99 %, ≤30 ppm MEHQ as inhibitor) were purchased from Sigma-Aldrich.

3 Depolymerization of unreinforced Elium 188O

This chapter will focus on the depolymerization of unreinforced Elium 188O and the reclaiming of the monomer in a small-scale setup. The goal is to demonstrate the feasibility of monomer reclamation. By analyzing reclaimed and residual material deeper knowledge about the overall process is generated.

3.1 Sample preparation

An amount of 500 g of Elium 188O was manually mixed for 5 mins with 3 wt% Luperox AFR 40. The formulation was then degassed for 5 min at -25 inHg (0.15 bar). In order to prevent boiling of the resin and evaporating of the highly volatile monomer (MMA) no full vacuum was applied. For the polymerization process the formulation was poured in an open glass mold in the size of 340 x 220 x 50 mm. After 24 h at ambient temperature, the mold was placed in a convection furnace (Heratherm OMH60, Thermo Fisher Scientific) for 24 h at 60 °C followed by 1 h at 80 °C. For the depolymerization process, the resulting plate with a thickness of 3-5 mm was cut with a band saw into cuboids with a side length of less than 20 mm.

3.2 Thermal degradation of Elium 188O

The thermal degradation behavior of polymerized Elium 188O was investigated by thermogravimetric analysis (TGA) on NETZSCH TG 209 F1 libra (Erich NETZSCH GmbH & Co. Holding KG). Therefore, aluminum oxide crucibles with a volume of 85 µL were used. The chamber was evacuated 3 times to avoid any O_2 during the measurement. Purge gas was N_2 with

a gas flow rate of 10 ml/min. The sample mass was recorded during heating from 24 to 650 °C with a heating rate of 5 K/min. Sample mass was between 11 and 14 mg and two samples were measured.

In Figure 1 a representative TGA curve of the non-isothermal mass loss of polymerized Elium 188O along with the mass derivative (-d*m*/d*T*) is shown (differential TGA (DTGA) curve). Two main degradation steps were observed with maximum -d*m*/d*T* at approx. 250 and 360 °C. This correlates with the proposed thermal degradation behavior of PMMA in the literature [13,14]. At 400 °C the sample was almost fully depolymerized and the sample mass was reduced to 1.5 ± 0.2%. At 650 °C only a small amount of residue (char) was left in the pans (0.7 ± 0.1%). It should be noted that this residue might also remain on the fibers during the depolymerization of composites with Elium 188O.

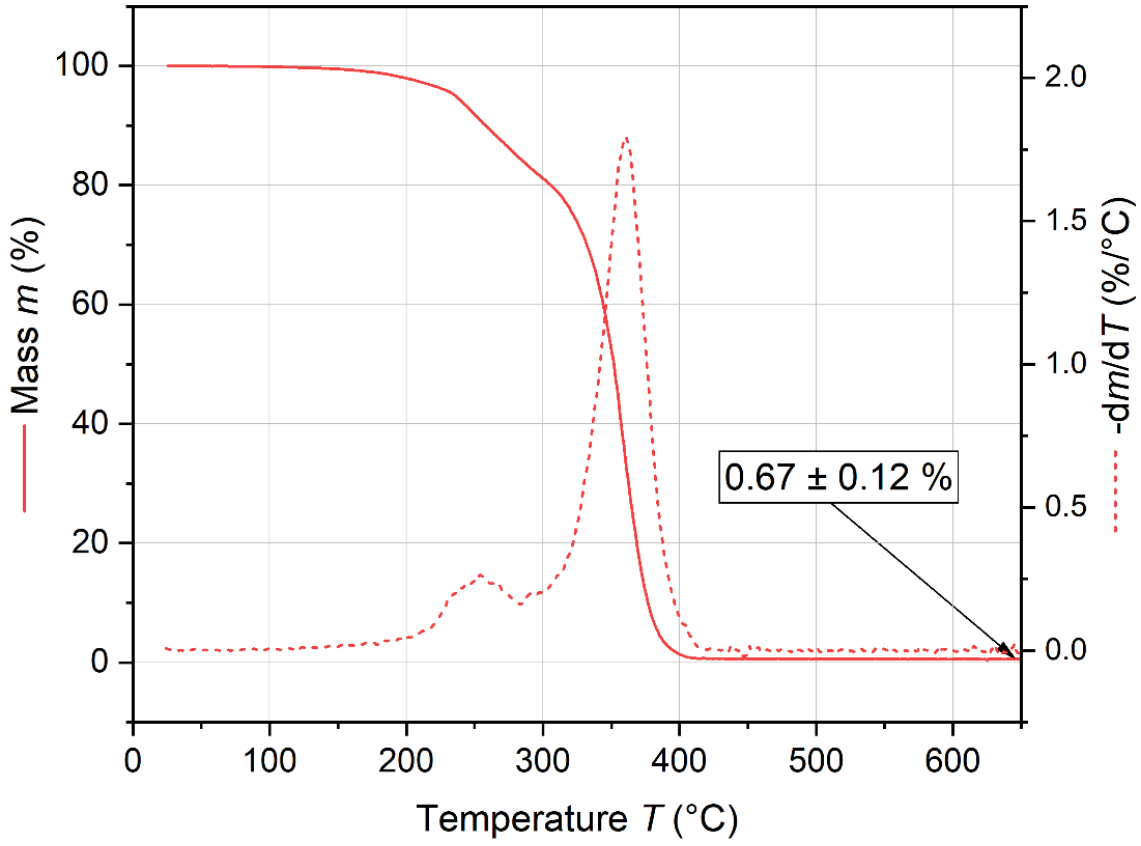

Figure 1: Representative TGA and DTGA curve of non-isothermal degradation of polymerized Elium 188O under N_2.

3.3 Depolymerization process

In Figure 2 the used setup for the small-scale depolymerization of Elium 188O and the reclaiming of the monomer is shown. Used components are listed in Table 1. The cut Elium 188O pieces were placed in a round bottom flask with 2 necks (depolymerization flask (1)), which was heated using a heating mantle (2). For thermal insulation the depolymerization flask was wrapped with glass wool (insulation is not shown in Figure 2). The temperature was monitored using a type-K thermocouple (3) with an 8-channel thermocouple data logger (TC-08) and PicoLog 6.2.7 software (Pico Technology). The thermocouple was placed between the bottom of the depolymerization flask and the heating mantle. A water-cooled condenser (4) at approx. 11 °C was used to condense the vapors. In order to prevent evaporation of the reclaimed monomer, the receiving flask was cooled with crushed ice to 0 °C (5). Oxidation was prevented by purging the system with N_2 with a flow rate of 150 - 170 mL/min (6-8). At the N_2 outlet (8) a glass beaker with water was placed to control the gas flow.

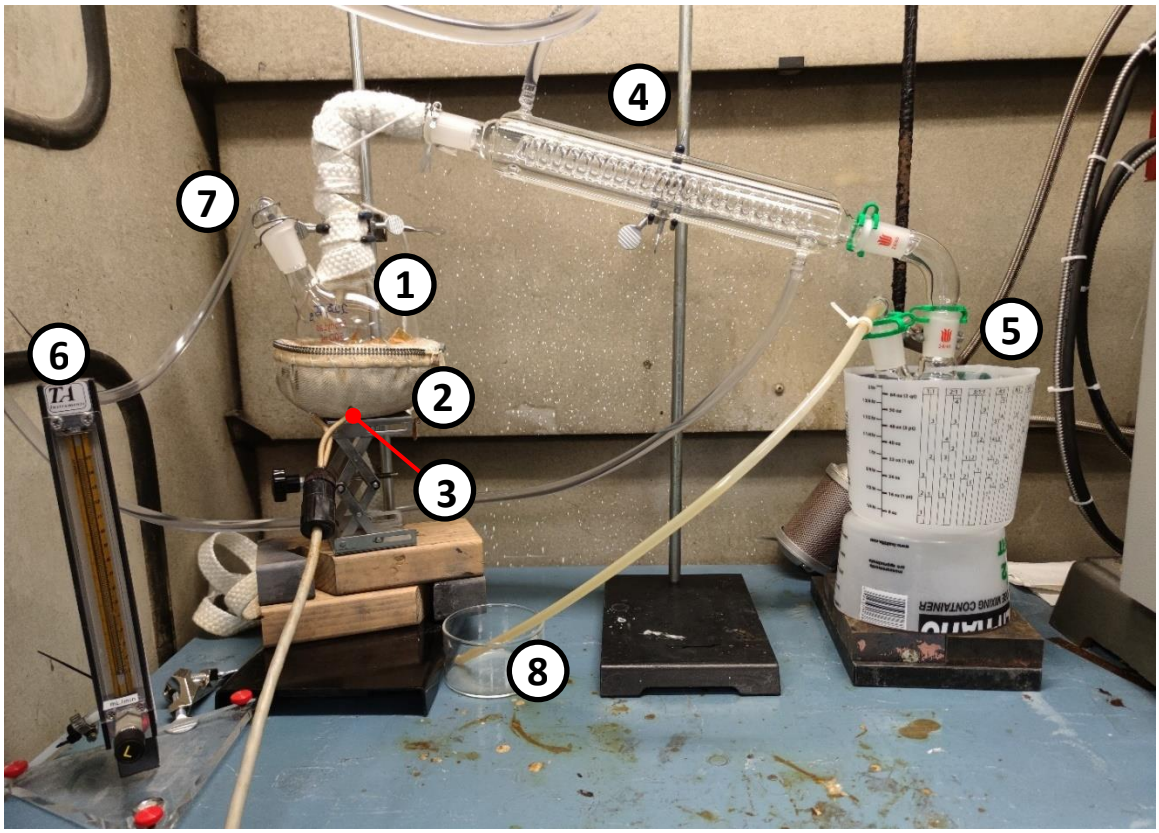

Figure 2: Setup for small-scale depolymerization and reclaiming of monomer.

Table 1: Used components for small-scale depolymerization and reclaiming of monomer.

Number	Component
1	Depolymerization flask (round bottom flask with 2 necks)
2	Heating mantle
3	Type K thermocouple
4	Condenser (water temperature 11 °C)
5	Receiving flask (round bottom flask with 2 necks: ice cooled at approx. 0 °C)
6	Flow meter
7	N_2 inlet
8	N_2 outlet

Two individual depolymerization experiments with a different amount of polymerized Elium 188O and different temperature profiles were performed (E1 and E2). The temperature ranged between 350 and 450 °C and was chosen based on the TGA results and previous work [12]. It should be noted that the temperature was manually regulated by adjusting the inlet voltage. Before the process was started, the system was flushed with N_2 for at least 10 min.

In the first depolymerization experiment (E1), 50 g of Elium 188O were used and the average temperature was approximately 410 °C for 5.5 h. In the second depolymerization experiment (E2), 100 g of Elium 188O were used and a step wise temperature profile was applied. First the system was heated to 350 °C for 1 h to ensure a uniform temperature. Then the temperature was increased to 400 °C for 3 h followed by a temperature of 450 °C for 1.5 h. The measured temperature during the experiments is shown in Figure 3. Small temperature fluctuations are related to adjustments of inlet voltage of the heating mantle and adjustments of the insulation material.

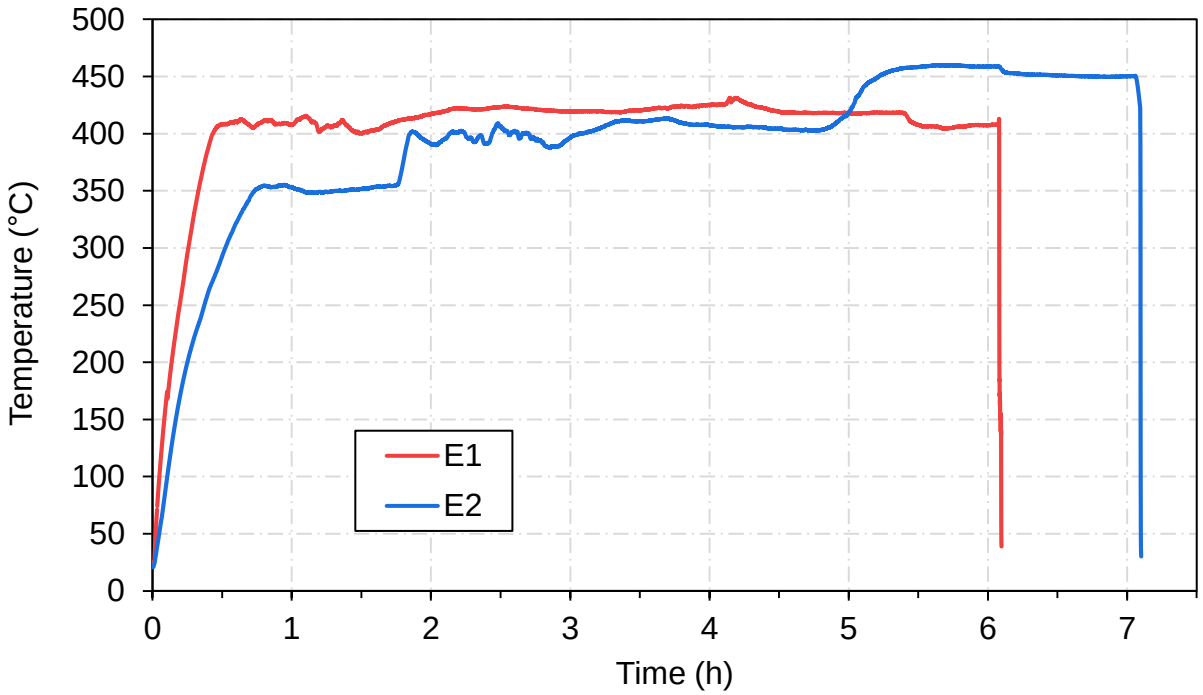

Figure 3: Monitored temperatures during the depolymerization experiments of unreinforced Elium 188O.

In Table 2 the results from both depolymerization experiments in term of mass of reclaimed resin, residues and losses are listed. These depolymerization products are shown in Figure 4. Between 72 and 81 % of the initial mass was reclaimed in the reclaiming flask after the depolymerization process. The reclaimed resin had a yellow color (Figure 4a) and was stabilized using 40-50 ppm MEHQ. In the depolymerization flask a residue fraction between 7 and 10 % of the initial mass persisted. This residue fraction contained a liquid (Figure 4b) and a solid phase (Figure 4c). During the process, condensing was observed at the top of the depolymerization flask, which reduced the amount of reclaimed resin and formed the liquid residue. In E2, this effect was reduced by the increased temperature (450 °C) segment at the end. Consequently, the fraction of liquid residue was smaller and the fraction of reclaimed resin was higher compared to E1. In E1 fraction of liquid residue was high enough to separate a small amount from the solid residue for further analysis. Both experiments showed a significant amount of losses between 13 and 18 %. This is mainly explained by a remaining liquid film in the distillation setup (condenser and adapter) but might also be connected to the evaporation of the monomer in the receiving flask. It should be noted that in the water used for monitoring the gas flow (Figure 2 – (8)) the smell of acrylate was

noticed. This indicates that, despite the cooling of the receiving flask, evaporation of the MMA was not completely avoided. Further it highlights the importance of proper cooling to maximize the amount of reclaimed resin and the MMA content.

Table 2: Results from depolymerization processes of Elium 188O.

No.	Initial Elium 188O mass	Reclaimed resin in receiving flask	Residue (liquid and solid) in depolymerization flask	Losses
1	50.27 g (100%)	36.42 g (72%)	4.88 g (10%)	8.97 g (18%)
2	99.92 g (100%)	80.54 g (81%)	6.53 g (7%)	12.85 g (13%)

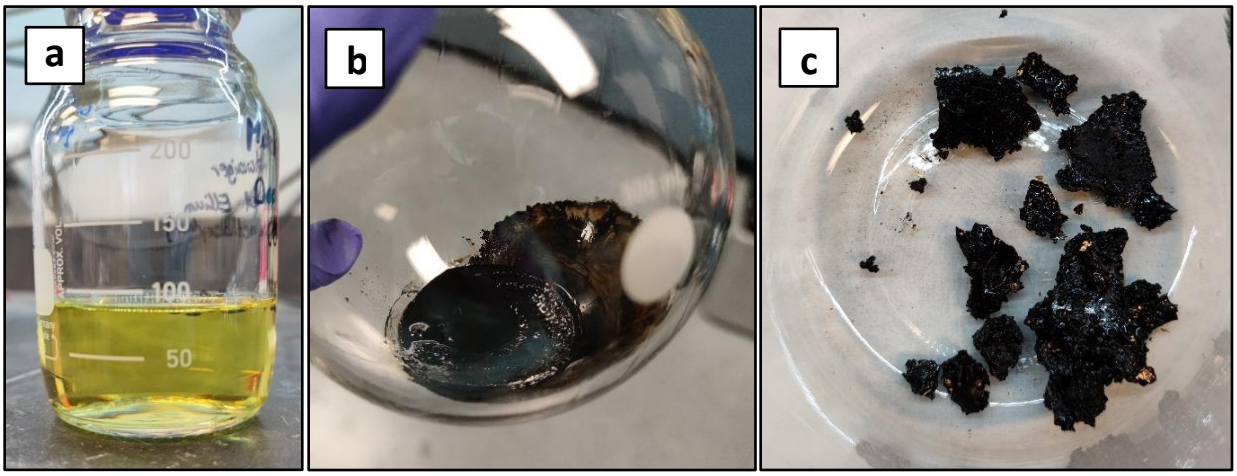

Figure 4: Depolymerization products of Elium 188O: a) reclaimed resin; b) liquid residue; c) solid residue.

3.4 Analysis of reclaimed resin and residues

3.4.1 Fourier-transform infrared spectroscopy

Reclaimed resins and liquid residue from the depolymerization process were investigated by Fourier-transform infrared spectroscopy (FT-IR) in attenuated total reflection mode. Spectra were recorded on the FT-IR/NIR spectrometer Spectrum 3 (Perkin Elmer Inc.) in the wavenumber range between 700 and 4000 cm^{-1} with a resolution of 4 cm^{-1}. In order to minimize the time for evaporation during measurement the scans per measurement were reduced to 4. For comparison purposes, the spectrum of pure MMA was measured. Each sample was measured at least 2 times. A spectrum of the liquid residue of E2 was not recorded because there was only a thin film on the solid residue.

In Figure 5 the spectra of MMA, reclaimed resins and liquid residue are shown. The prominent absorbance band in MMA at 1722 cm^{-1} and 1639 cm^{-1} are related to the C=O stretching of ester and C=C stretching, respectively [15]. Both absorbance bands were also found in the reclaimed resins. This verifies the successful depolymerization and the presence of MMA. Overall, beside some minor additional absorbance peaks, the spectrum of the reclaimed resin from E1 was almost identical to the spectrum of MMA. The additional absorbance peaks might be the result from the formation of by-products during depolymerization or due to evaporation of other components in the Elium 188O. Absorbance bands at 1767 and 1677 cm^{-1} are attributed to the C=O stretching of different molecules, i.e. different esters carboxylic acids or aldehydes. This absorbance bands were even more pronounced for the reclaimed resin from E2, suppressing the characteristic MMA absorbance bands. Furthermore, changes in the range between 3100 and 2800 cm^{-1} (CH and CH_2 stretching) as well as additional absorption bands in the fingerprint region were observed. This indicates the presence of more additional components compared to E1 which is explained by the increased depolymerization temperature.

The liquid residue from E1 showed even more additional absorbance bands compared to the spectra of reclaimed resins. The broad absorbance band in the range between 3600 and 3250 cm^{-1} is related to OH stretching, indicating the presence of alcohol. Additional shoulders at the ester band of MMA (1722 cm^{-1}) can be observed at 1800 and 1705 cm^{-1}. Those are again connected to C=O stretching of different molecules (anhydrides, different esters, ketones, aldehydes). Overall, this findings correlates with the by-products found by Bel Haj Frej et al. [10], who reported methanol, different acrylates, esters and acids in the reclaimed resin. Elium 188O also contains 1-5% aldehyde according to its SDS. It can be concluded that the liquid residue contained the most by-products beside MMA.

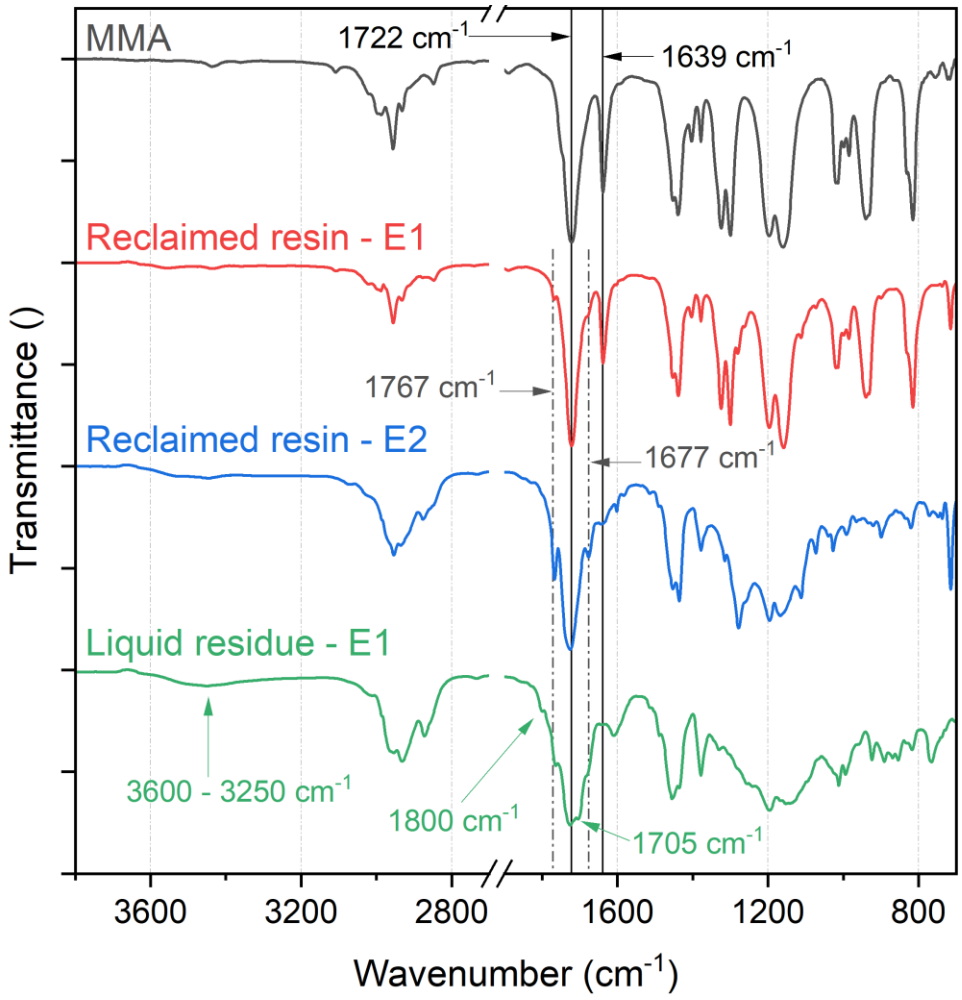

Figure 5: FT-IR spectra of pure MMA, reclaimed resins and liquid residue after depolymerization of Elium 188O.

3.4.2 Gas chromatography with flame ionization detection

Quantification of the MMA content in the reclaimed resin was performed by gas chromatography with flame ionization detection (GC-FID). Measurements were performed on a HP Agilent 6890A Series GC-FID system (Agilent Technologies). Dodecane was used as internal standard and acetonitrile was used as solvent. Injection volume was 1 µL and the used carrier gas was He (pressure of 62.6 psi, 95.9 mL/min). The temperature range was between 40 and 250 °C with a heating rate of 50 K/min. For the calibration curve a stock solution of dodecane (2.30 mg/L) and MMA (2.83 mg/L) was prepared with 10 mL acetonitrile. An amount of 0.50 mL of the dodecane stock solution was then mixed with 0.25, 0.50, 0.75, 1.00 or 1.25 mL of the MMA stock solution.

In Figure 6 the calibration curve for MMA with dodecane is visualized. A good linear correlation (R^2 = 0.997) between the mass ratio (MMA/dodecane) and the area content ratio was achieved. The amount of MMA in the reclaimed resin was then calculated following Equation (1), whereas *m* is the mass of dodecane and reclaimed resin in the sample and *A* is the integrated area of the detector response of MMA and dodecane, respectively.

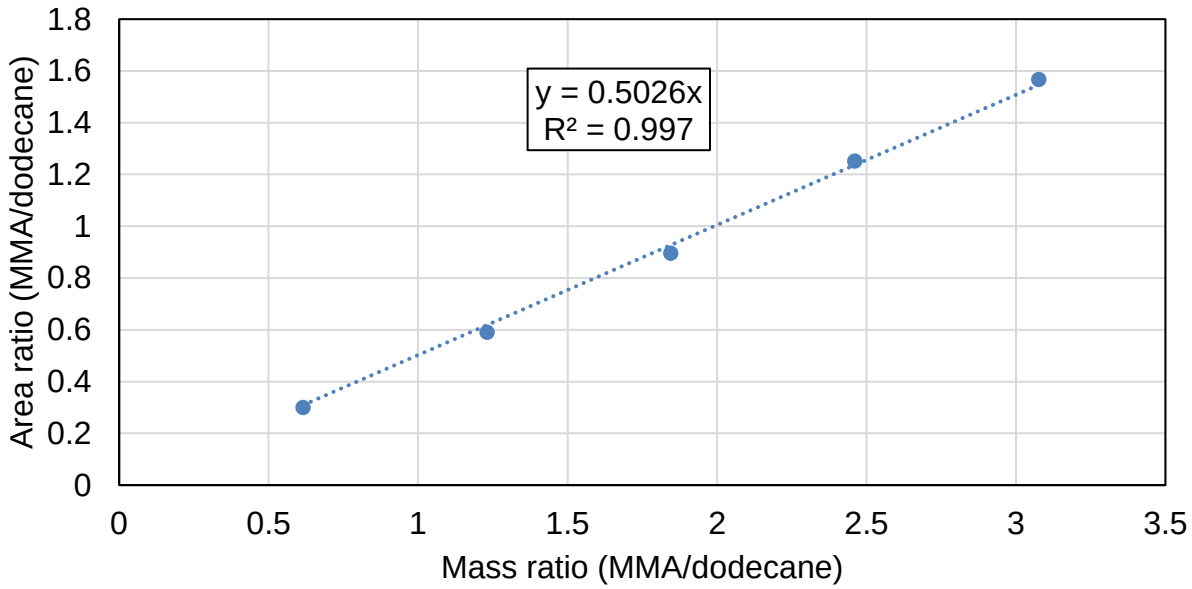

Figure 6: Calibration curve for GC-FID measurements with MMA and dodecane as internal standard.

$$MMA\ content\ (\%) = \frac{100\%}{0.5026} * \frac{\rho_{dodecane}}{\rho_{reclaimed\ resin}} * \frac{A_{MMA}}{A_{dodecane}} \qquad (1)$$

For sample preparation, around 34 mg of reclaimed resins were diluted with 5 ml acetonitrile. An amount of 0.25 mL of this solution was then mixed with 0.25 mL of dodecane in acetonitrile (2.66 mg/L). In Table 3 the resulting masses in the prepared samples, the GC-FID results and calculated MMA content are summarized. The calculated MMA content in the reclaimed resin was between 77 and 72%. The lower MMA content of the reclaimed resin from E2 correlates with the findings from FT-IR measurements as it exhibited more additional absorption bands in the spectrum. Based on the amount of reclaimed resin, the total amount of reclaimed MMA was between 55 and 58%. However, as mentioned in chapter 3.3 the smell of acrylate was noticed

during the polymerization. Thus, it is likely that the measured MMA content was smaller because some MMA already evaporated during the depolymerization process. In addition, some MMA could also have evaporated in the time period between the depolymerization step and the GC-FID measurement (4-5 weeks).

Table 3: Amount of dodecane and reclaimed resin from Elium 188O depolymerization in the GC-FID samples along with GC-FID results and calculated MMA content.

No.	$m_{reclaimed\ resin}$ (mg)	$m_{dodecane}$ (mg)	A_{MMA} ()	$A_{dodecane}$ ()	MMA content in reclaimed resin (%)
E1	1.705	0.665	294.1	295.7	77
E2	1.695	0.665	258.6	280.2	72

3.4.3 Thermogravimetric analysis

The solid residues of the two depolymerization experiments were investigated by thermogravimetric analysis (TGA) on the NETZSCH TG 209 F1 libra TGA. Purge gas was N2 with a gas flow rate of 10 ml/min and aluminum oxide crucibles with a volume of 85 µL were used. The sample mass was recorded during heating from 24 to 770 °C with a heating rate of 5 K/min. Sample mass was between 14 and 22 mg. Three measurements were performed per sample.

In Figure 7 the resulting TGA curves of the solid residues are visualized. All samples showed a similar behavior with small differences in the amount of mass loss at certain temperatures. This is related to different fractions of remaining liquid residue on the solid residues. Mass loss was observed in the temperature range between 400 and 550 °C and between 400 and 550 °C. The first mass loss is related to evaporation of the liquid residue. The second mass loss might be attributed to the depolymerization of residual Elium 188O components, indicating that the polymerization was not fully completed. At 770 °C there was still between 42 and 57% of the material which indicates that most of the solid residue is presumable char.

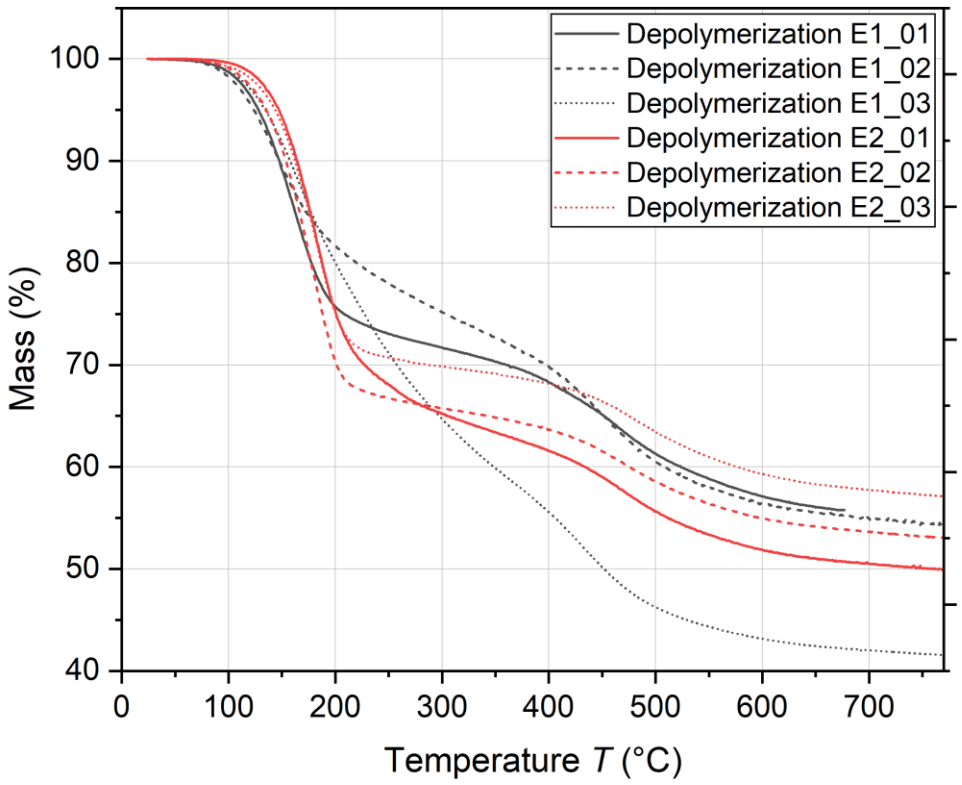

Figure 7: TGA curves of the solid residue from depolymerization E1 and E2 of Elium 188O under N_2.

3.4.4 Solvent tests

Observed residues might also remain on the fibers when recycling composites [10], even though the residue amount is significant smaller. It is assumed that particularly liquid residue may cause recycled fibers to stick together. This will result in dispersion problems of fibers which is crucial for the alignment of short fibers [12]. Thus, the efficacy of typical organic solvents was investigated to remove the liquid residue from the solid residue. For this purpose, between 17 and 24 mg of the solid residue was mixed with > 1 mL of solvent in 0.5 dram glass vials and stored at ambient temperature for 24 h.

In Table 4 the used organic solvents are summarized along with the visual behavior after 24 h. Additionally, the discoloration of the transparent solvents is visualized in Figure 8. Despite their different classification, acetone, isopropanol, tetrahydrofuran and toluene showed dark discoloration of the solvents indicating the solubility of the liquid residue. Methanol and Hexane showed only a slight discoloration, while for distilled water no color change was observed. The solid residue itself was not soluble in any of the solvents, as would be expected with char.

Table 4: Used organic solvents for removal of liquid residues

No	Solvent	Classification	Visual behavior after 24 h
1	Acetone	Polar aprotic	Dark discoloration of solvent
2	Isopropanol (lab. grade)	Polar protic	Dark discoloration of solvent
3	Tetrahydrofuran (99%)	Polar aprotic	Dark discoloration of solvent
4	Toluen (99.9%)	Non-polar aprotic	Dark discoloration of solvent
5	Methanol (99.9%)	Polar protic	Slight discoloration of solvent
6	Hexane (97%)	Non-polar aprotic	Slight discoloration of solvent
7	Distilled water	Polar protic	No color change, residue floats on water

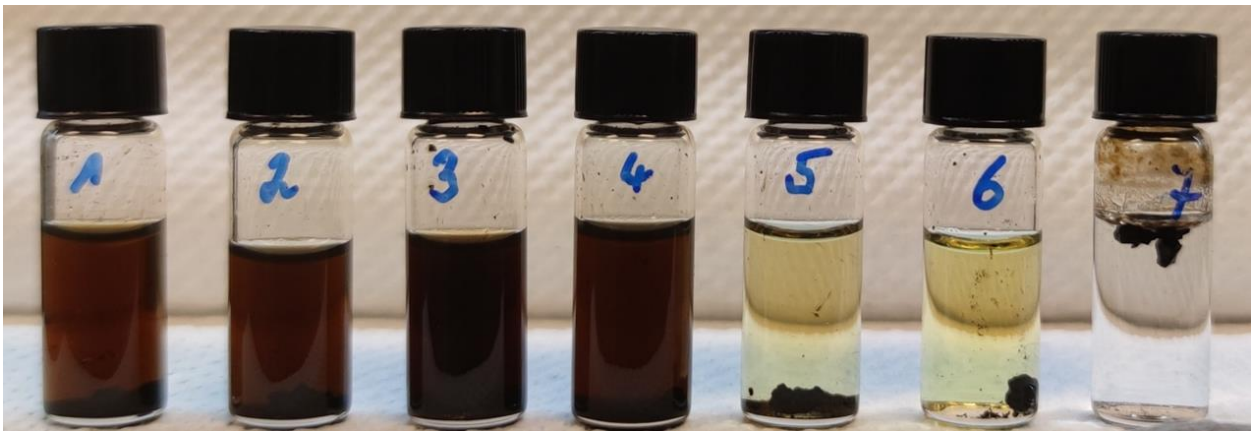

Figure 8: Discoloration of the organic solvents after 24 h at ambient temperature.

Based on these results, isopropanol was chosen for cleaning the solid residue in a rinsing process. Isopropanol proved to be effective and it is the solvent with the least harmful effect on health. In Figure 9 this rinsing process is visualized. First, 67.10 mg of solid residue was washed and distributed in isopropanol (Figure 9a). After mixing for 5 min with a glass stick, the solid residue was filtered under vacuum using a paper filter. Then it was rinsed several times with isopropanol until no more discoloration of the solvent was observed (Figure 9b). Overall approximately 75 mL of isopropanol were used. After drying the filter for 24 h at 40 °C the mass of the solid residue was 30.76 mg (46% of initial mass) and the solid residue particles were not sticky anymore (Figure 9c). This result correlates with the residual mass in TGA measurements. Concluding, isopropanol is a suitable solvent to wash away the liquid residue.

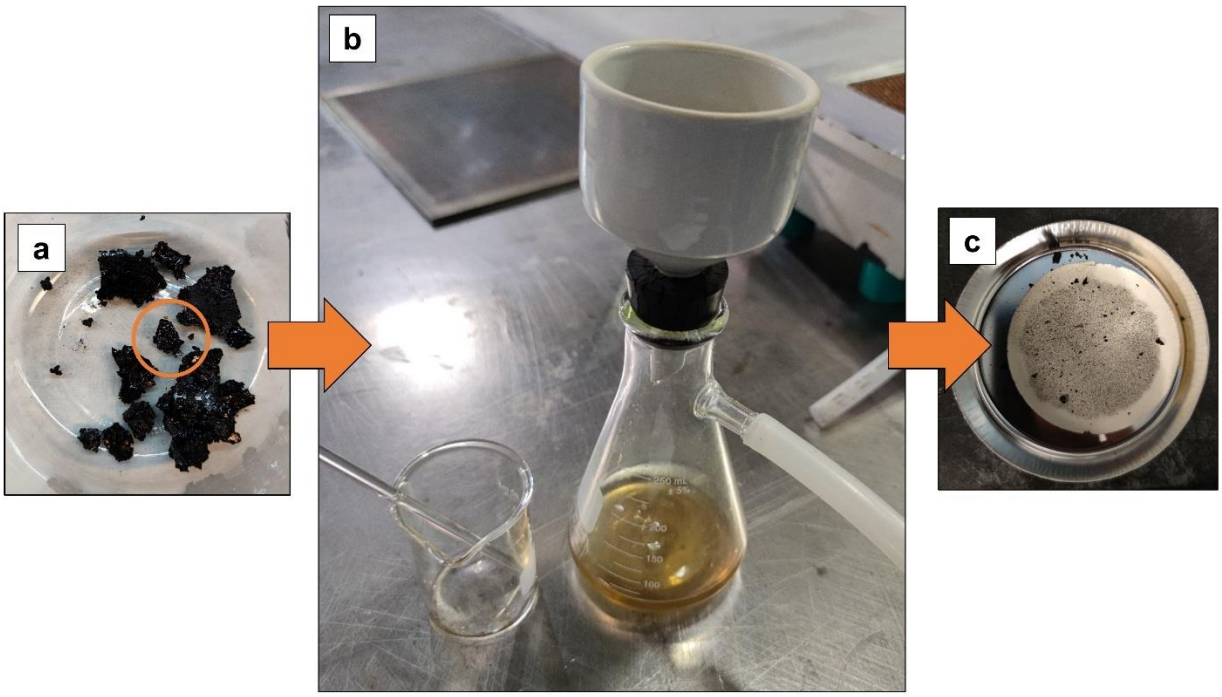

Figure 9: Rinsing process of solid residue with isopropanol: a) unwashed solid residue, b) filtering and rinsing setup, c) dried solid residue particles.

4 Depolymerization of composites

In the following chapter the recycling of composites from TuFF material is addressed. This includes the reclaiming of the resin, as already demonstrated in previous chapter 3, as well as the reclaiming of the carbon fibers. The small-scale depolymerization setup was optimized in 3 different steps by using 2 different composite panels. Further, the reclaimed fibers are investigated and possible ways for cleaning are addressed.

4.1 Composite no. 1

4.1.1 Composite manufacturing

As reinforcement TuFF feedstock from IM7 carbon fibers (fiber length of 3 mm) were used. A number of 64 layers in the size of 6 x 6 in (152 x 152 mm) were centrically placed on top of 40 layers in the size of 7 x 8 in (178 x 203 mm). The used layers with variating sizes were selected based on availability and to maximize the amount of composite. The composite was

manufactured by using a Vacuum Assisted Resin Transfer Molding (VARTM) process. In Figure 10 the full VARTM setup is schematically shown, whereas an infusion guide for Elium 188O provided by Arkema was followed. The metal plate was coated with a release agent (LOCTITE® FREKOTE 55NC, Henkel Corporation). An amount of 300 g of Elium 188O was used and prepared as described in chapter 3.1. A vacuum of approximately -25 inHg (0.15 bar) was applied during the first polymerization cycle (24 h at 60 °C). Then the composite was demolded and the post annealing step was performed in a convection furnace (Heratherm OMH60, Thermo Fisher Scientific) for 24 h at 60 °C and 1 h at 80 °C. It should be noted that during infusion air leak was noticed. However, since the composite is only used for recycling purposes, this was not further considered.

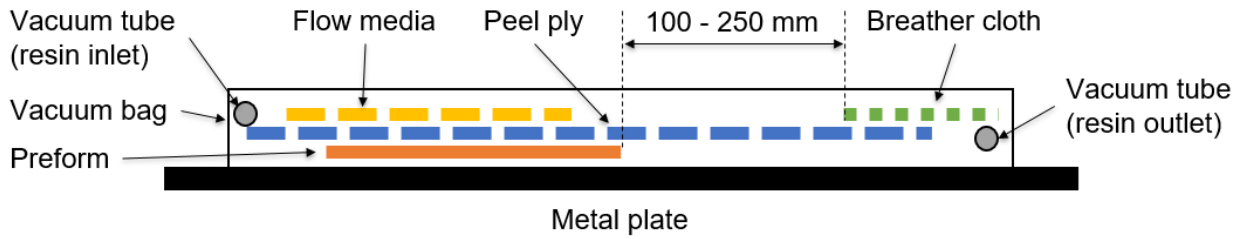

Figure 10: VARTM setup for TuFF feedstock infusion with Elium 188O.

In Table 5 the mass, densities (given by manufacturer) and calculated volume of fibers and resin are listed. Additionally, the fiber weight fraction and the fiber volume fraction were calculated. The fiber weight fraction was 52.3% and will be used for the further calculations. The fiber volume fraction was 41.6%, which is higher than reported values for VARTM process with TuFF feedstocks (25-30%, [12]). This is explained by the occurred air leaks which led to infusion problems. Nevertheless, the composite was perfectly suitable for recycling purposes. For the depolymerization process the composite was cut into rectangular pieces with a side length smaller than 70 mm using a water-cooled circular saw. Before the depolymerization process the composite parts were dried at 50 °C for 24 h.

Table 5: Mass, densities and volume of fibers and resin in composite no. 1.

Material	Mass (g)	Density (g/cm³)	Volume (cm³)
IM7 fibers	22.32	1.80	12.40
Elium 188O	20.37	1.17	17.41
Total	42.69		29.81
		Fiber weight fraction	**52.3%**
		Fiber volume fraction	**41.6%**

4.1.2 Depolymerization process

In Figure 11 the used reaction kettle for the depolymerization process of the composite is shown. The round bottom flask was replaced by a 500 mL reaction kettle with three necks. In the bottom a stainless-steel grid was inserted to ensure better air circulation and to separate fibers from possible residual resin. The prepared composite sheets were then placed stacked on this grid (Figure 11b). Overall, despite the depolymerization flask, the same setup as shown in Figure 2 was used. Oxidation was prevented by purging the system with N_2 with a flow rate of 150 mL/min and before the process the setup was flushed with N_2 for at least 10 min. It should be noted that the overall volume of the reaction kettle with lid was approximately between 1200 and 1250 ml.

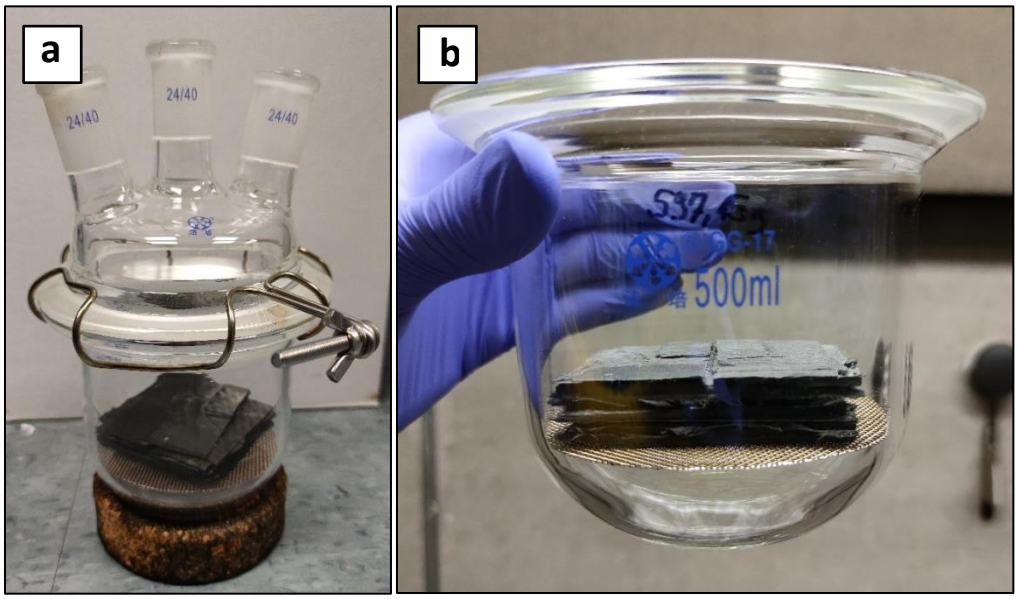

Figure 11: Reaction kettle for small-scale depolymerization of composite: (a) overview; (b) bottom part with inserted stainless-steel grid and stacked composite.

In total two thermal runs (run 1 and run 2) were applied on the composite no. 1 with two different setups as schematically shown in Figure 12. In run 1, only the heating mantle was used to heat the round part of the bottom reaction kettle part (setup 1). The temperature was monitored using thermocouples between the depolymerization flask and the heating mantle on the bottom and on the side. Despite the thermal insulation, the heat loss was too high for proper depolymerization. While the bottom temperature was 416 °C, the side temperature was 326 °C (average values over 6 h after 1 h heating). Accordingly, the real temperature at the composite was presumable even lower than 326 °C and in the total time of 6 h only 23% of the Elium 188O in the composite depolymerized.

Therefore, a second run (run 2) was performed where the bottom reaction kettle part was additionally heated with a fiberglass heater tape (STH102-080, Omega Electric). In order to track the real temperature at the composite an additional thermocouple was placed inside the kettle flask (setup 2) and the neck was sealed with high temperature sealing tape (A8003G, Airtech International). The heating mantle and the fiberglass heater tape were controlled separately. The monitored temperatures in run 2 with setup 2 are shown in Figure 13. After 2 h heating, the temperature at the composite was constant and kept at an average value of 398 °C for 4 h. Overall, the temperature was above 360 °C for 5 h (maximum of mass derivative in TGA curve as shown in Figure 1).

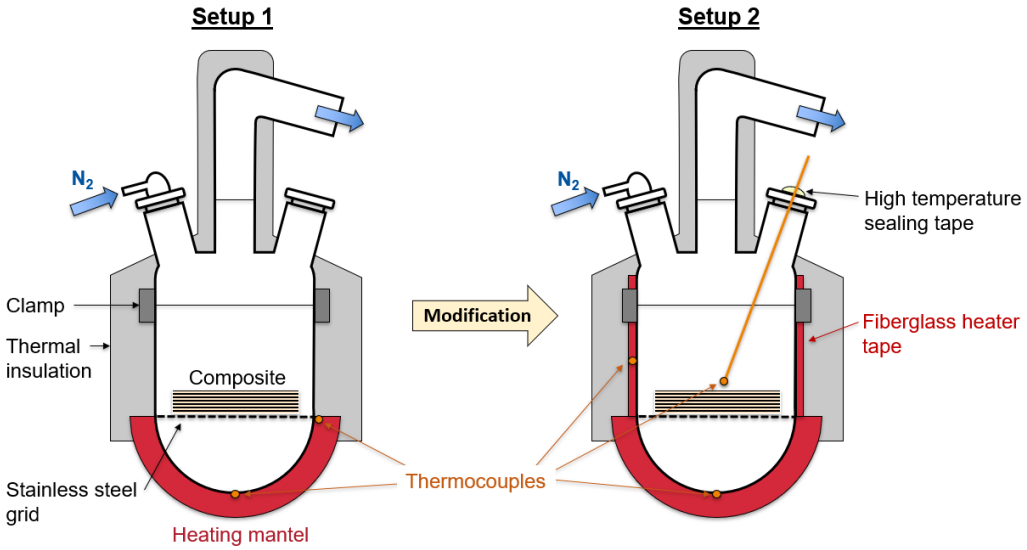

Figure 12: Depolymerization setup 1 and 2 for the small-scale depolymerization of composites.

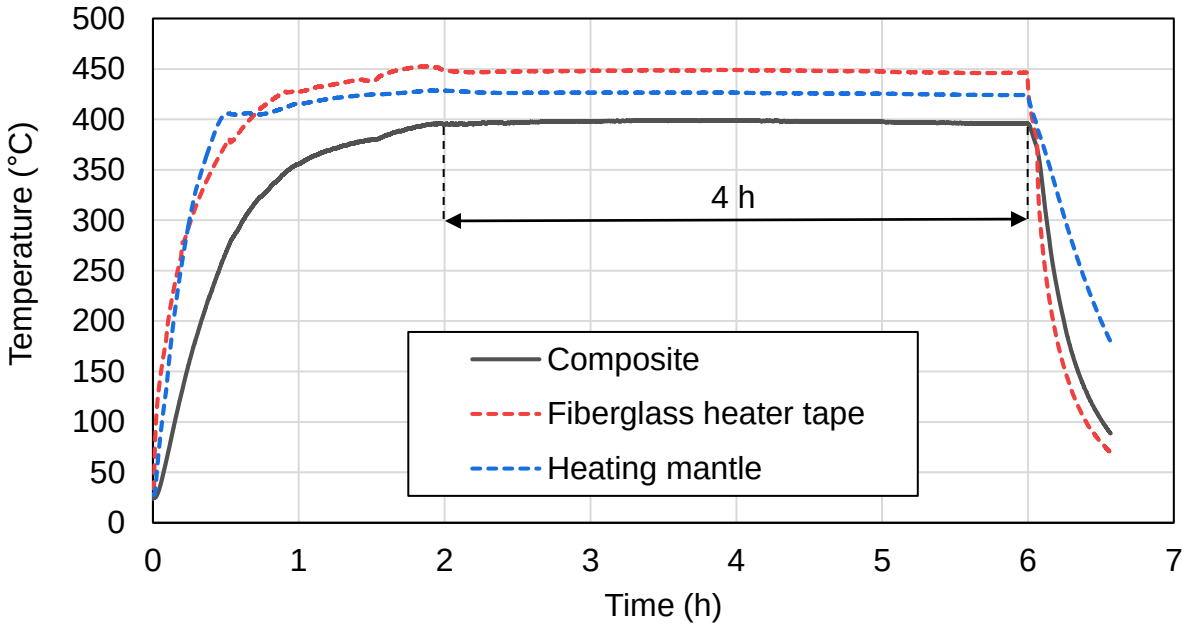

Figure 13: Monitored temperatures during the depolymerization run 2 of composite no. 1.

The results of the depolymerization process are summarized in Table 6. After run 2 with setup 2, the total mass loss of Elium 188O in composite no. 1 was 95% and 49% of the initial mass was reclaimed. The relative high amount of losses (45%) is explained by the small amount of Elium 188O and the two individual runs. Between the two runs, which both showed a remaining liquid film in the condenser and adapter, the whole setup was cleaned which further increased the total amount of losses. However, the absolute losses were smaller than the experiments with unreinforced Elium 188O. The reclaimed resin was darker compared to the reclaimed resin from unreinforced Elium 188O and had orange-brownish color as shown in Figure 14a. After depolymerization the bottom part of the reaction kettle showed no residual traces of depolymerization products, whereas the top part was discolored as visualized in Figure 14b. However, no residual liquid resin was found in the reaction kettle which indicates that condensation of depolymerized resin in the reaction kettle was avoided by the additional heating source and the isolation.

Table 6: Results from depolymerization process of composite no. 1.

	Before depoly-merization	Run 1 (setup 1)	Run 2 (setup 2)	Total	Total amount in relation to Elium 188O mass before depolymerization
Composite (g)	40.17	35.57	22.15	-	-
Elium 188O in composite (g)	19.17	14.57	1.05	-	5.5%
Amount of depolymerized Elium188O (g)	0.00	4.59	13.52	18.11	94.5%
Reclaimed resin (g)	0.00	1.28	8.16	9.44	49.3%
Losses (g)	0.00	3.31	5.36	8.67	45.2%

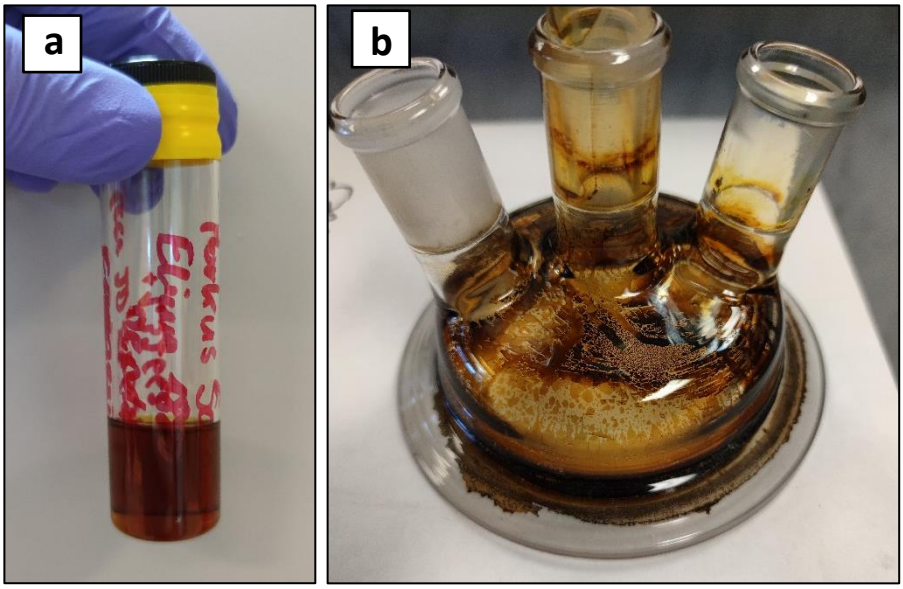

Figure 14: Reclaimed resin from depolymerization of composite no. 1 in (a) and discoloration of top part of reaction kettle after depolymerization in (b).

Due to the theoretical amount of 5% residual resin on the reclaimed fibers after the depolymerization, the fibers still stuck together. This is visualized in Figure 15 by deforming the reclaimed fiber panels. When bending in fiber direction (Figure 15a) the fiber panel was still very stiff and the fiber held together. After releasing the force, the panel deforms back to its initial flat shape. In contrast, the fiber panel can be easily bended transverse to fiber direction (Figure 15b), as there is not enough resin to provide stiffness. Transverse to fiber direction, fibers could be pulled apart by hand (Figure 15c). In contrast, this was not possible in fiber direction which also indicates bonding between the fibers.

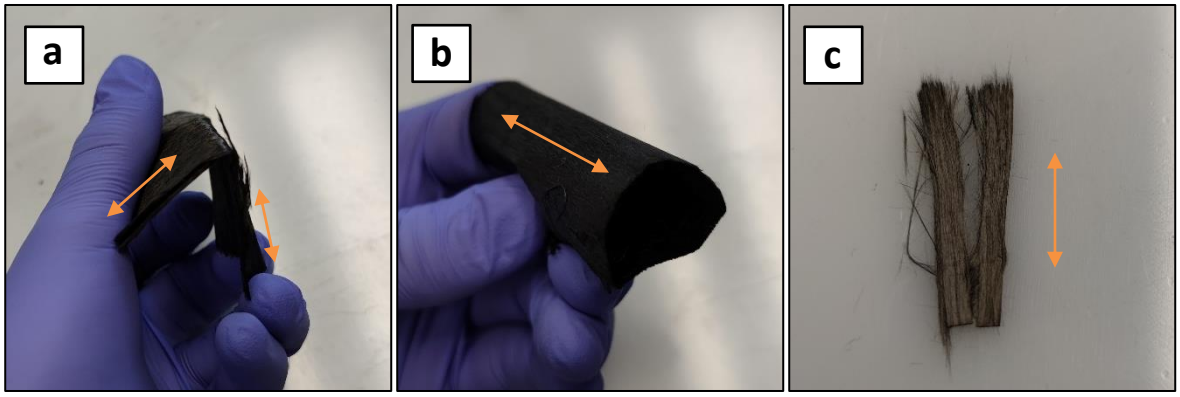

Figure 15: Deformation behavior of reclaimed fiber panels from composite no.1: (a) bending in fiber direction, (b) bending transverse to fiber direction), (c) fibers pulled apart transverse to fiber direction. Orange arrow indicates the fiber direction.

4.1.3 Thermal post processing

Due to amount of residual resin in the reclaimed fiber panel, an additional thermal post processing was applied to investigate the effect of a higher depolymerization temperature. This was performed on one fiber panel (mass of 4.233 g) after depolymerization run 2. Since there is only a small amount of resin left, which can be barely reclaimed in the given depolymerization setup due to the amount of losses, this was performed in an annealing furnace (GLO 40/11-1G from Carbolite Gero Ltd). The furnace was evacuated and purged with N_2 three times to minimize the presence of O_2. The gas flow rate of N_2 was 500 l/h, which is comparable to the previously used gas flow rate when compared to the total furnace or reactor volume. The furnace was heated to 450 °C for 1 h with a heating rate of 5 K/min. The sample was placed on a metallic grid to allow a better gas flow. It should be noted that the gas flow in the GLO furnace is generally better compared to the small-scale depolymerization setup, because the composite is placed between gas inlet and outlet, which are on the opposite sites. In contrast, in the small-scale depolymerization setup both are on the top of the reaction kettle which cause turbulences.

The mass loss of the fiber panel after this thermal post processing was 0.7 %. Further, there was no difference in the deformation behavior and the fibers still stuck together. Thus, there was still residual material which held the fibers together and the higher temperature of 450 °C did not significantly improve the fiber quality after depolymerization. Also, it is not clear if the mass loss

is only attributed to the higher temperature or to the better gas flow. Therefore, a second composite was manufactured and an optimized depolymerization process was applied.

4.2 Composite no. 2

4.2.1 Composite manufacturing

Due to availability, TuFF feedstocks from T700-3M carbon fibers (fiber length of 3 mm) were used for the second composite (no. 2). These fibers have a slightly larger fiber diameter (7 µm instead of 5.2 µm). A number of 24 layers in the size of 7 x 8 in (178 x 203 mm) were used. The composite was manufactured using a bladder molding process, which was proven in achieving better composite qualities with better consistency. In Figure 16 the used setup is schematically shown. The bottom part of the mold was coated with a release agent. After preparing Elium 188O as described in chapter 3.1, the mold was closed and the pressure in the upper mold was increased to 200 psi (13.8 bar). The infused was started by applying a vacuum of -20 inHg (0.3 bar) and the infusion pressure was increased up to 50 psi (3.4 bar). The Elium 188O was polymerized for 4 h at ambient temperature and post cured at 80 °C for 2 h. This shorter polymerization cycle was given by Arkema and was proven to result in the same material properties.

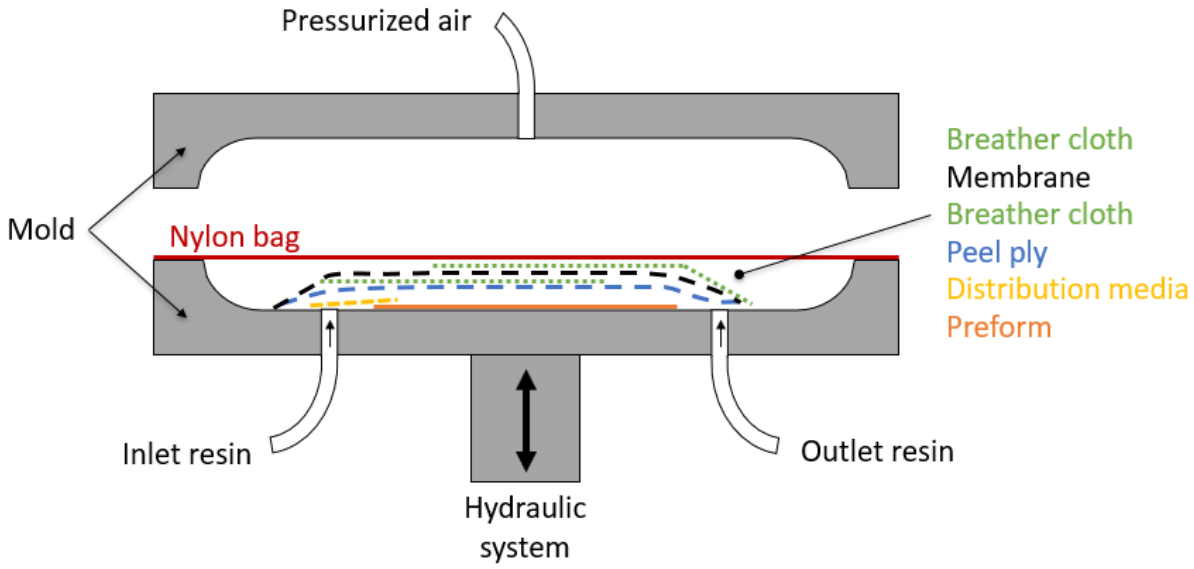

Figure 16: Bladder molding setup for TuFF preform infusion with Elium 188O.

The manufactured composite had an average thickness of 0.29 mm. In Table 7 the mass, densities and calculated volume of fibers and resin are listed. Additionally, the resulting fiber weight fraction and the fiber volume fraction were calculated. The fiber weight fraction was 47.9% and the fiber volume fraction was 41.6%. For the depolymerization process the composite was cut into 9 rectangular pieces in the size of approximately 60 x 65 mm using scissors.

Table 7: Mass, densities and volume of fibers and resin in composite no. 2.

Material	Mass (g)	Densities (g/cm^3)	Volume (cm^3)
T700-3M fibers	5.60	1.80	3.11
Elium 188O	6.08	1.17	5.20
Total	11.68		8.31
Fiber weight fraction			**47.9%**
Fiber volume fraction			**37.4%**

4.2.2 Depolymerization process

During the depolymerization of composite no. 1, three main points were identified for further improvement. The N_2 inlet and outlet were both on the top of the reaction kettle, which might result in a bad gas flow to remove the depolymerized resin. This was addressed by using a gas inlet with extended tube to introduce the gas below the composite panels. Also, it is assumed that the stacking of the individual panels disturbed the gas exchange. Therefore, 0.4 mm thin stainless-steel grids were used to separate the panels in the reaction kettle. As last step, the used depolymerization temperature was addressed. As demonstrated earlier (Figure 1), 400 °C is already above the depolymerization peak temperature. Therefore, an isothermal segment at 350 °C for 1 h was added before the 400 °C step which should decrease depolymerization rate in the beginning and decrease the amount of formed char. The optimized setup 3 is schematically visualized in Figure 17 and the monitored temperature is shown in Figure 18. After 2 h heating, the temperature at the composite was constant with an average value of 349 °C for 1 h. Then the system was heated to 400 °C within 30 min and kept at an average temperature of 401 °C for 3 h.

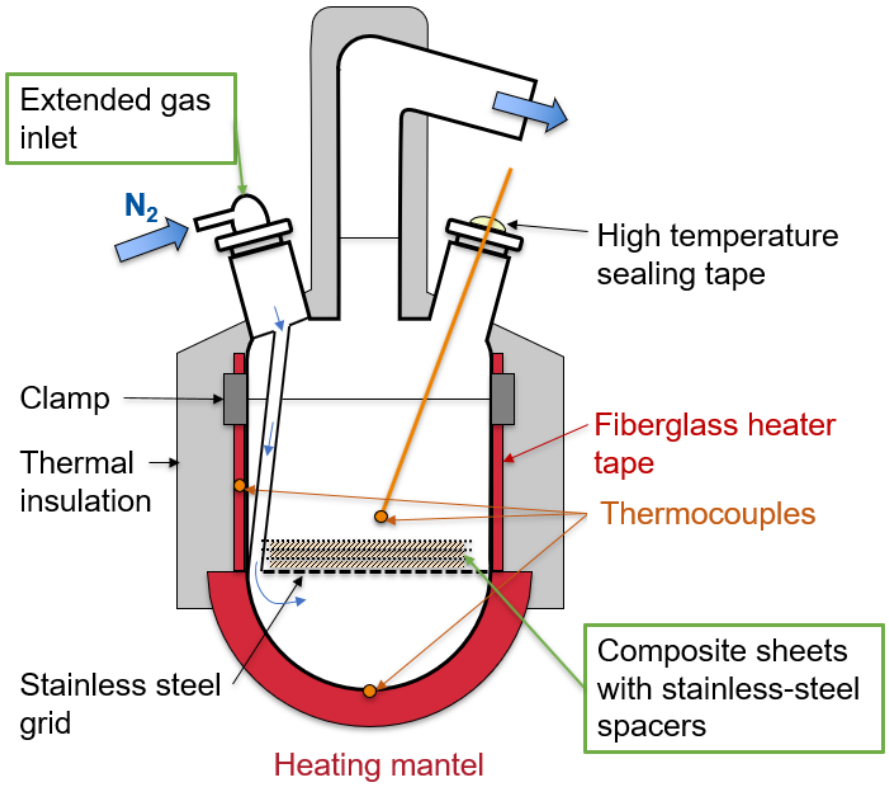

Figure 17: Optimized depolymerization setup 3 for the small-scale depolymerization of composites with changes highlighted in green.

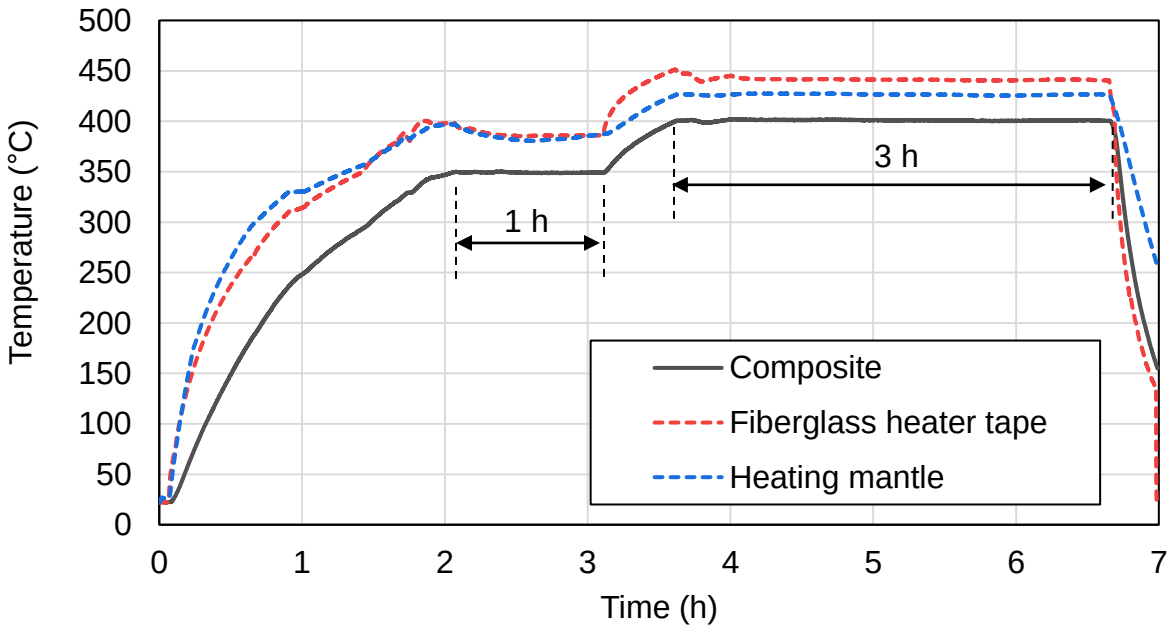

Figure 18: Monitored temperatures during the depolymerization of composite no. 2.

The results of the depolymerization process are summarized in Table 8. An amount of 97% of the Elium 188O in the composite was depolymerized and 45% of the initial mass was reclaimed. Again, the high amount of losses (52%) is explained by the small amount of initial Elium 188O in the composites. Overall, the absolute amount of losses (3.0 g) is in the same range as for composite no. 1 (between 3.3 and 5.4 g per run).

The residual resin in the composite (3% of initial weight weight) was only slightly lower compared to the depolymerization of composite no. 1. Accordingly, the fibers also stuck together after the depolymerization. There was much less discoloration of the reaction kettle, which might be attributed to the lower initial amount of Elium 188O and/or to the lower depolymerization temperature in the first step. Further, also the reclaimed resin was less dark and more yellowish comparable to the reclaimed resin in chapter 3.3.

Table 8: Results from depolymerization of composite no. 2.

	Before depolymerization	After depolymerization	Amount after depoly. in relation to Elium 188O mass before depoly.
Composite (g)	11.19	5.54	-
Elium 188O in composite (g)	5.82	0.18	3.0%
Depolymerized Elium 188O (g)	0.00	5.65	97.0%
Reclaimed resin (g)	0.00	2.62	45.0%
Losses (g)	0.00	3.03	52.0%

4.3 Analysis of reclaimed resin

4.3.1 Fourier-transform infrared spectroscopy

The FT-IR spectra of the reclaimed resin from the depolymerization of the two composites were recorded as described in chapter 3.4.1. For composite no. 1, the reclaimed resin of both depolymerization runs (run 1 and 2) were analyzed. However, it should be noted that in run 1 the temperature at the composite was unknown. In Figure 18, the recorded spectra are shown and compared to the spectrum of pure MMA. As for the depolymerization of the unreinforced Elium 188O, the presence of MMA can be verified by the absorbance bands at 1722 cm^{-1} and 1639 cm^{-1},

which are attributed to the C=O stretching of ester and C=C stretching, respectively. However, for composite no. 1 the C=C bands were overlapped by many other absorbance bands and not that prominent, which might indicate a lower MMA content. Again, several additional peaks were observed at 1800, 1767, 1703 and 1675 cm^{-1} which are attributed to the formation of several by-products exhibiting C=O groups. Overall, the spectra of the resin from the depolymerization of composite no. 2 showed the fewest additional absorbance bands and was most similar to the spectra of MMA. It can be concluded, that MMA was successfully reclaimed during the depolymerization of the composites.

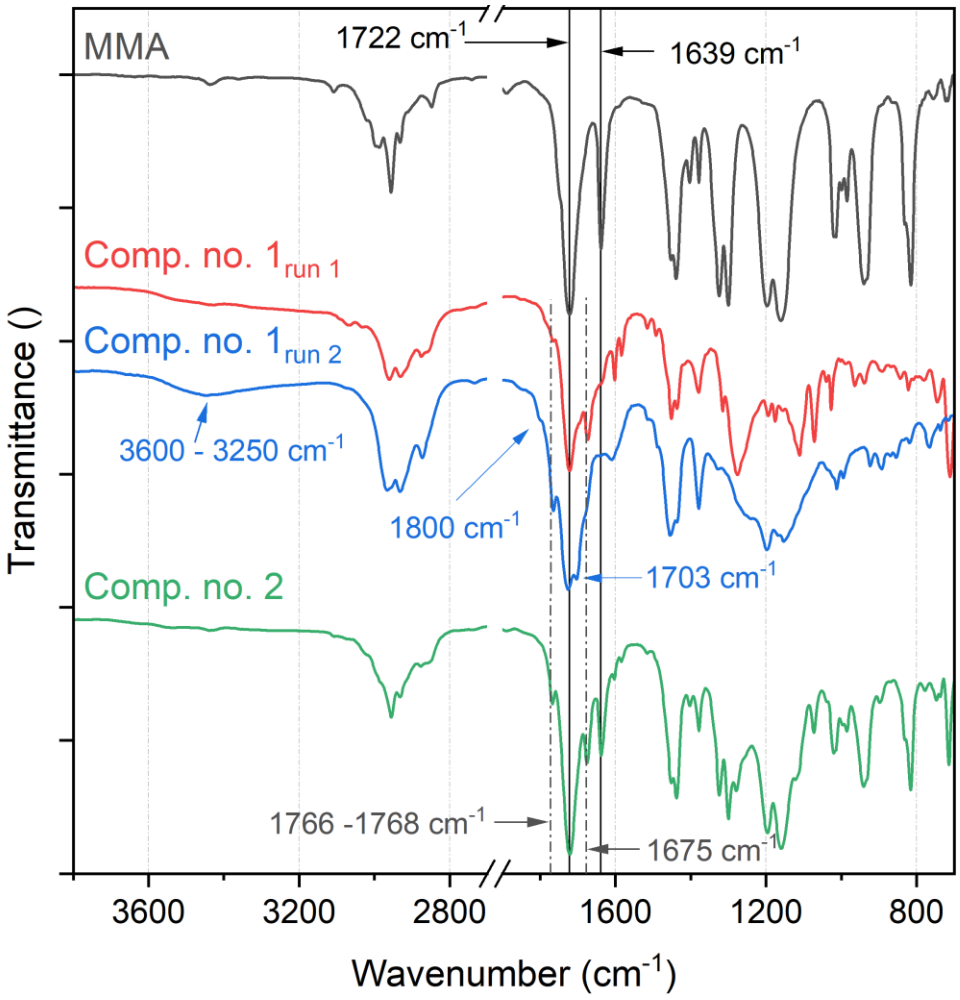

Figure 19: FT-IR spectra of pure MMA and reclaimed resins from the depolymerization processes on composite no. 1 and 2.

4.3.2 Gas chromatography with flame ionization detection

The GC-FID measurements were performed and evaluated as described in chapter 3.4.1. Samples for the determination of the MMA content using GC-FID were prepared in a similar manner. Between 63 and 72 g of the reclaimed resins were diluted with 10 ml acetonitrile. An amount of 0.5 mL of the dilute reclaimed resin was then mixed with 0.5 mL of dodecane in acetonitrile (2.66 mg/L). In Table 9 the resulting masses in the prepared samples, the GC-FID results and calculated MMA content are summarized. The calculated MMA content was between 8 and 88%. The reclaimed resin from composite no. 1 after run 1 exhibited only a small MMA content of 8%, while after run 2 the MMA content was 66%. Based on the weights of the reclaimed resin after the individual runs (see Table 6) this results in total amount of 58% MMA in the reclaimed resin of composite no. 1. The reclaimed resin of composite no. 2 exhibited an MMA content of 88%, which is even higher than for the depolymerization of unreinforced Elium 188O. This high MMA content is attributed to the controlled stepped depolymerization procedure (1 h at 350 °C and 3 h at 400 °C), but also to the better gas flow in the setup. Thus, with an optimized depolymerization setup and temperature profile, not only more wt% of Elium 188O is depolymerized but also a much higher MMA content is achieved.

Table 9: Amount of dodecane and reclaimed resin from composite depolymerization in the GC-FID samples along with GC-FID results and calculated MMA content.

Composite sample	$m_{\text{reclaimed resin}}$ (mg)	m_{dodecane} (mg)	A_{MMA} ()	A_{dodecane} ()	MMA content in reclaimed resin (%)
No. 1 – run 1	3.61	1.33	29.7	279.6	8
No. 1 – run 2	3.19	1.33	226.5	284.2	66
No. 2	3.23	1.33	288.0	269.4	88

4.4 Analysis of reclaimed fibers

In the TuFF process, the single fibers can only be aligned when they are dispersible in water without forming fiber bundles. The dispersibility of the fibers can be tested with a simple test developed by the Center for Composite Materials (CCM). Herein, a pinch of fibers is mixed with 600 mL of water in a 1000 mL glass beaker in a fiber-water volume ratio of 1:37.500. After stirring

for 10 min with 400 rpm, the mixture is inspected for the existence of fiber bundles or clumping and the dispersibility of is evaluated.

An overview of the investigated reclaimed fibers is given in Table 10 with the applied temperatures in the depolymerization process. For simplification, composite no. 1 states only the depolymerization temperature of run 2, because in run 1 only a small amount was depolymerized which is assumed to be not relevant for the reclaimed fibers. None of the fibers were dispersible in water, which is exemplarily shown in Figure 20 for the fibers from composite no. 1 after the thermal post processing. Additionally, the effect of washing in isopropanol and THF on the dispersibility of the fibers was investigated based on the result from the solvent tests. Therefore, approximately 0.03 g of the fibers were mixed with 150 mL of solvent for 1 h with 400 rpm. However, neither isopropanol nor THF showed any improvement of the dispersibility. Therefore, the fibers were further analyzed using TGA and a scanning electron microscope (SEM). Washed fibers were filtered and rinsed three times with 50 mL of fresh solvent to wash away any contamination on the surface.

Table 10: List of reclaimed fibers with used depolymerization temperatures.

Composite	Fibers	Depolymerization process	Note
No. 1	IM7	4 h at 400 °C	Small-scale setup (run 2)
		4 h at 400 °C + 1 h at 450 °C	Small scale setup (run 2) + GLO furnace (thermal post processing)
No. 2	T700-3M	1 h at 350 °C + 3 h at 400 °C	Small scale setup with optimized N_2 gas flow

Figure 20. Example of non-dispersible reclaimed fibers in water.

4.4.1 Thermogravimetric analysis

The amount of residual resin on the reclaimed fibers were measured using TGA following the same procedure described as in 3.2. The sample mass was between 29 and 31 mg and for each depolymerization process two or three samples were measured.

In Figure 21 the resulting TGA curves of the reclaimed fibers are shown. The small mass loss before 100 °C is attributed to the evaporation of water. A second mass loss, which might be related to the depolymerization of residual resin, was observed above 400 °C with a maximum mass loss rate between 500 and 550 °C. At 650 °C fibers from composite no. 1 after 4 h at 400 °C showed a mass loss of 0.7%. This is significantly smaller than the calculated residual Elium 188O of 5.5% in the composite (see Table 6). The difference may be explained by the formation of char during the depolymerization, which remain on the fibers but is not removed under N_2 at given temperatures. The amount of 4.8% of char is significantly higher than the amount of char during depolymerization of Elium 188O in the TGA (0.7%). By using the thermal post processing (+ 1 h at 450 °C), the mass loss at 650 °C was slightly decreased to 0.5%. However, this small difference could also be attributed to local variations.

Fibers from composite no. 2 showed a lower mass loss of 0.4% at 650 °C, which is again smaller than the calculated residual Elium 188O of 3.0% in the composite (see Table 6). Overall, these results might indicate that with the depolymerization process of composite no. 2 not only less residual resin remains on the fibers, but also less char is formed. Furthermore, it is revealed that the additional thermal post processing is not that effective to remove the remaining resin and probably even higher temperatures are required.

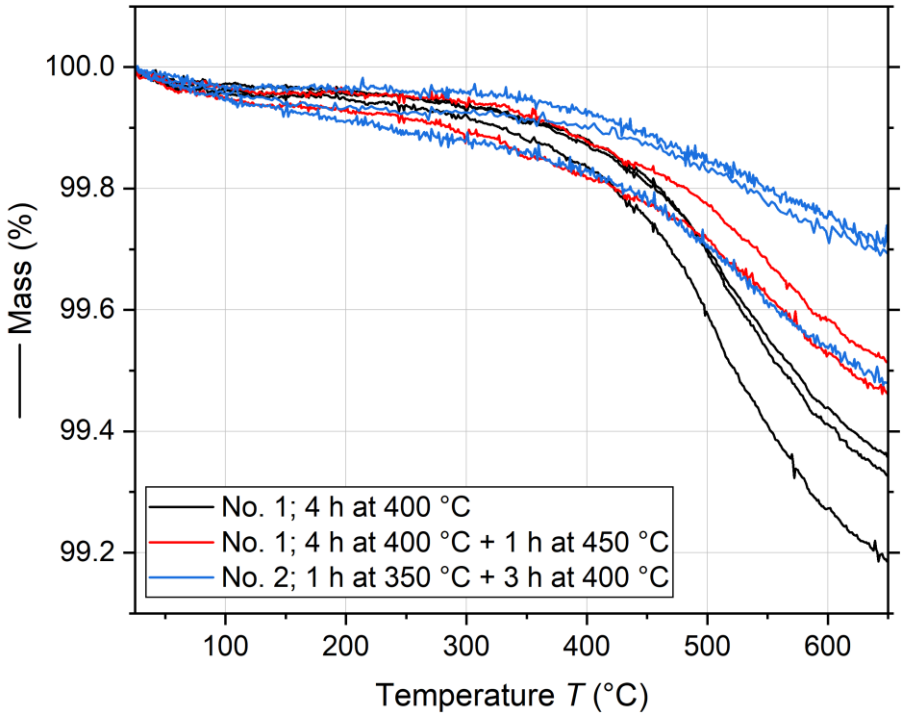

Figure 21: TGA curves of the reclaimed carbon fibers under N_2.

4.4.2 Scanning electron microscopy

The surface of the reclaimed fibers was analyzed with a TM-1000 tabletop SEM (Hitachi). The fibers were placed on the sample holder using a carbon tape. In Figure 22 selected SEM images of these fibers are depicted. Fibers from composite no. 1 exhibited many particles (Figure 22a) which are likely residues from the depolymerization (residual resin or char). Washing with a solvent (either isopropanol or THF) reduced the number of particles which is exemplarily shown for isopropanol in Figure 22b. Also, the thermal post processing reduced the number of particles as shown in Figure 22c. This agrees with the measured weight loss of 0.7% and with the TGA measurements.

Fibers from composite no. 2 also exhibited less particles compared to the fibers from no. 1. Thus, in accordance with the weight measurements and TGA results, the optimized depolymerization process improved the quality of the reclaimed fibers without any post treatment. However, all fibers were still contaminated with residuals and were not dispersible.

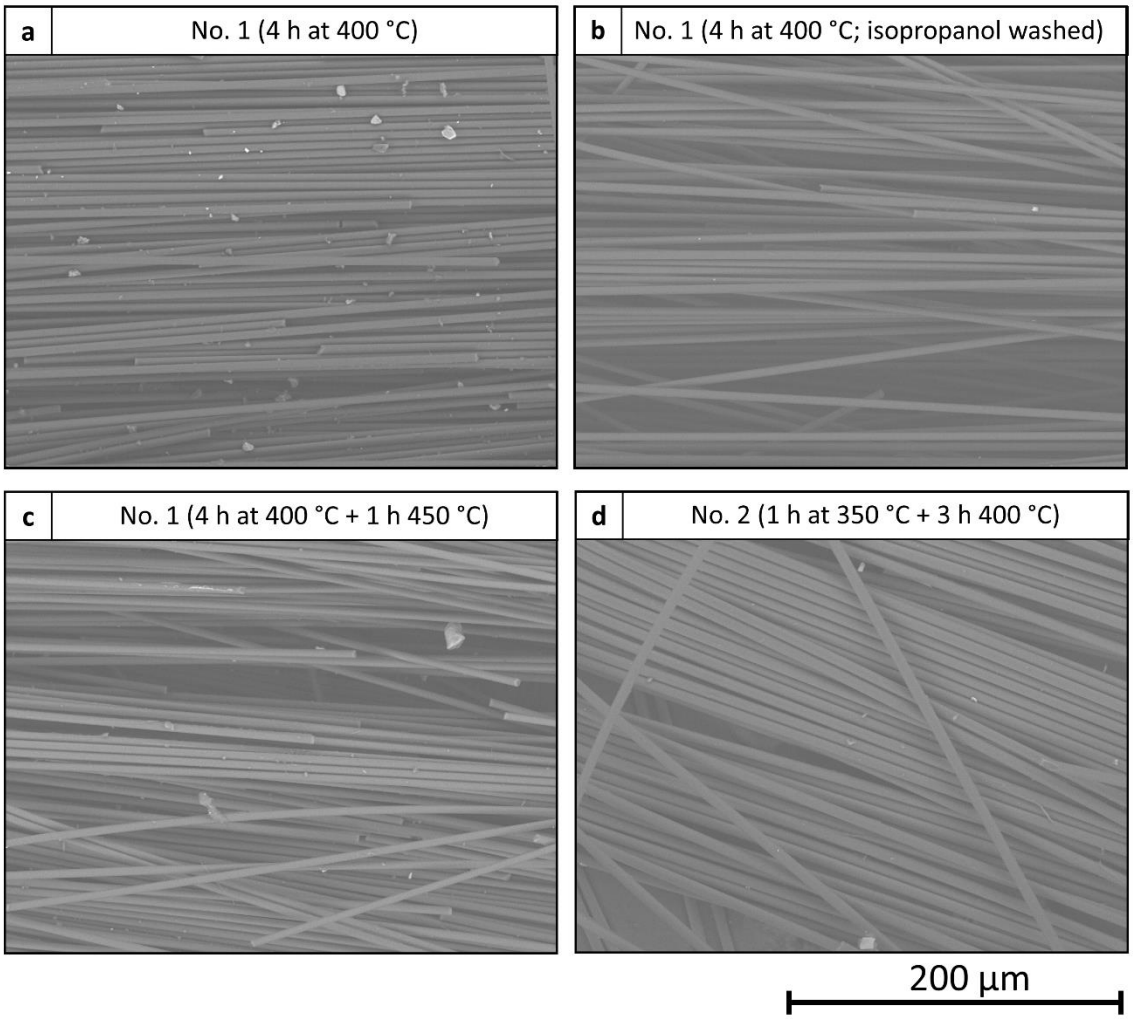

Figure 22: SEM images of reclaimed carbon fibers (magnification of 500x).

To analyze fibers more in detail, isopropanol washed fibers of composite no. 1 and no. 2 were additionally investigated with another SEM (ZEISS Auriga 60, Carl Zeiss AG), which allows to take images with better resolution at a higher magnification. Therefore, fibers were gold sputtered using the CCU-010 compact coating unit (safematic GmbH).

As exemplarily visualized in Figure 1Figure 23a, the fibers exhibited some residue patches on the surfaces. Besides some smaller residue patches, most of them formed “longitudinal and discontinuous ridges” as also observed by Bel Haj Frej et al. [10]. Further, in some areas with oriented fibers, residue was observed between the fibers which is exemplarily shown in Figure 23b. Especially this residue, presumable residual resin, causes the fibers to stick together and make them non-dispersible in water. Since this residue was not removed with solvents or at higher temperatures under N_2 atmosphere, other ways to obtain clean and dispersible fibers need to be explored. It should be noted that the residue on the fibers was not deeper analyzed. However, identification of the residue using Energy Dispersive X-Ray or nanoscale IR spectrometer might be useful in the future to further develop a cleaning process or optimize the depolymerization.

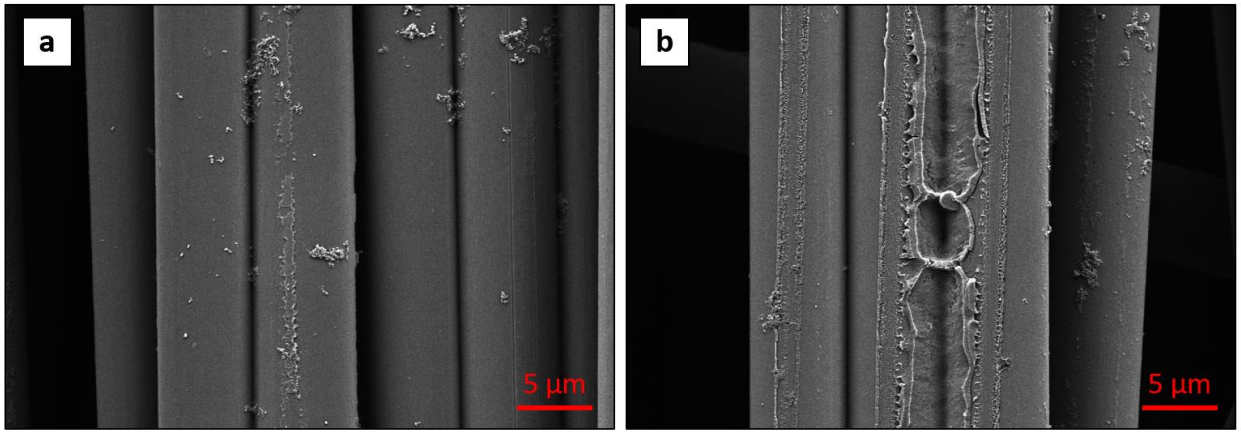

Figure 23: SEM images of reclaimed carbon fibers from composite no. 2 after washing with isopropanol (magnification of 5000x).

4.4.3 Oxidation under air

In order to evaluate possible ways to further clean the reclaimed fibers and make them dispersible, the effect of oxidation at evaluated temperatures under air was investigated. Therefore, approximately 0.03 g of fibers were placed in alumina oxide crucibles. These samples were then put in a pre-heated muffle oven at 450 °C under air for 10, 15, 20 or 25 min. After cooling down, the dispersibility of the fibers in water was tested which is shown in Figure 24 for composite no. 1.

Big fiber bundles were still present after 10 or 15 min. After 20 min, most of the fibers were dispersible and only a few smaller fiber bundles were present. After 25 min, the fibers were fully dispersible. This is also confirmed under a light microscope (KEYENCE VHX-6000 with dual-objective lens VH-ZST, Keyence Corporation). No fiber bundles were detected as shown in Figure 25. Thus, by adding an additional depolymerization step under air, fibers, which are suitable to produces new TuFF preforms from recycled, can be reclaimed. However, it should be noted that the required oxidation time to receive dispersible fibers will also depend on the given gas flow in the process and the thickness of the fiber panels. The oxidation time needs to be optimized for the given process and should be kept as short as possible to reduce a loss in tensile strength [16,17].

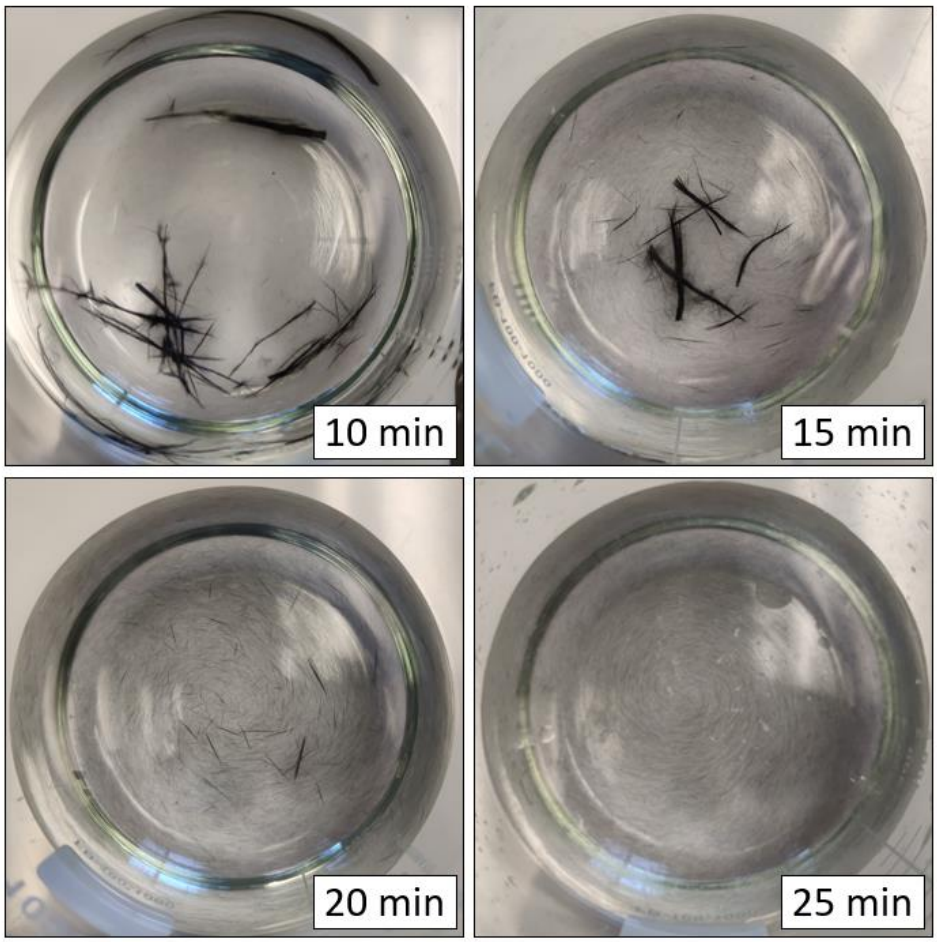

Figure 24: Dispersibility of fibers from composite no. 1 after thermal treatment for 10, 15, 20 or 25 min at 450 °C under air.

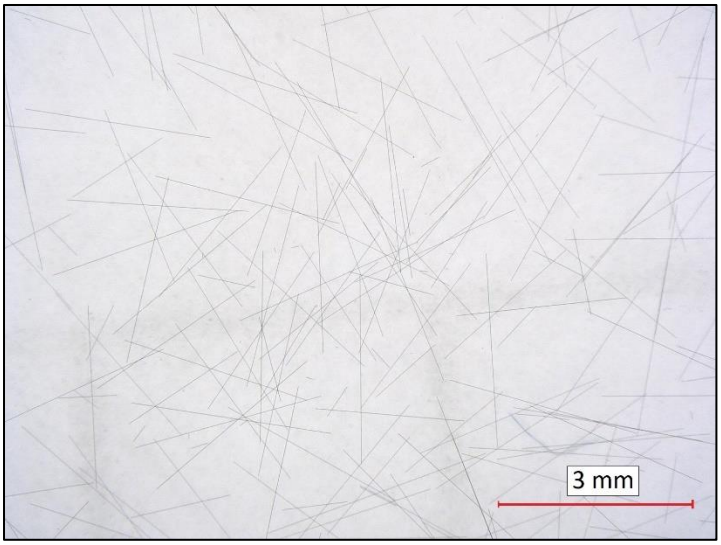

Figure 25: Dispersibility of fibers from composite no. 1 after 25 min at 450 °C under light microscope with magnification of 30x.

5 Reuse of reclaimed resin without further processing

This chapter investigates the reuse of reclaimed without any further processing i.e. distillation to receive pure MMA and formulating into new Elium 188O. The aim is to evaluate if a small amount of crude reclaimed resin can be added to Elium 188O without any losses in terms of mechanical and thermal properties. By using the crude reclaimed resin energy is saved and no new petrochemical based material are required.

5.1 Sample preparation

A total amount of 6 g was prepared by mixing 80% of Elium 188O (4.8 g) with 20% of reclaimed resin from E1 (1.2 g, MMA content of 77%). The formulation was manually mixed for 3 mins with 3 wt% Luperox AFR 40 and degassed for 3 min at -25 inHg (0.15 bar). For comparison purposes a formulation with 100% Elium 188O and a formulation with Elium 188O (80%) mixed with pure MMA (20%) were prepared in the same way. The space between two glass plates (100 x 75 mm) separated with a 1 mm thick PTFE sealing on three sides was used as casting mold. The final obtained cavity was 70 x 70 x 1 mm. Inner surfaces of the cavity were coated with a release agent two times (Chemlease R&B EZ, Chem-Trend L.P.). The cavity was filled with the prepared

formulations and purged with N_2 before sealing with a tape. Purging with N_2 was done to remove O_2 which acts as a polymerization inhibitor. The same temperature procedure as described in chapter 3.1 was applied. The used mold and a representative Elium 188O plate with a thickness of 1 mm are visualized in Figure 26.

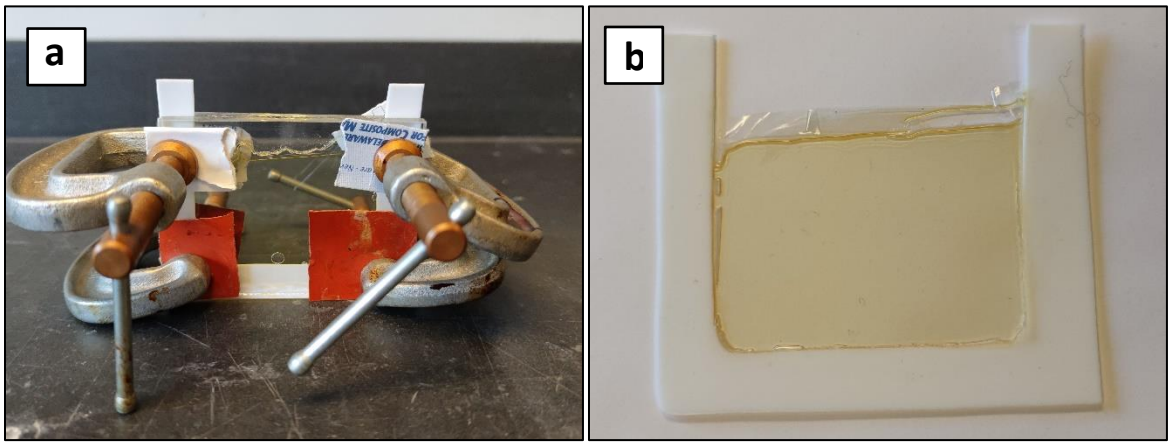

Figure 26: Used mold for casting plates (a) and demolded polymerized Elium 188O sample (b).

5.2 Fourier-transform infrared spectroscopy

FT-IR spectra of the polymerized Elium 188O samples were recorded on the FT-IR/NIR spectrometer Spectrum 3 in attenuated total reflection mode in the wavenumber range between 700 and 4000 cm^{-1}. The resolution was 4 cm^{-1} and 16 scans per measurement performed. Two measurements were performed for each sample.

In Figure 27 representative spectra of the polymerized Elium 188O samples are shown. Overall, no significant differences in absorption bands were detected. Thus, no effect of the added reclaimed resin or MMA on the polymerization was observed by FT-IR. Nevertheless, all samples show a very small reaming peak between 1636 and 1638 cm^{-1}. As described in chapter 3.4.1, this absorption band is attributed to the C=C stretching. This indicates that in all samples unreacted C=C groups were present.

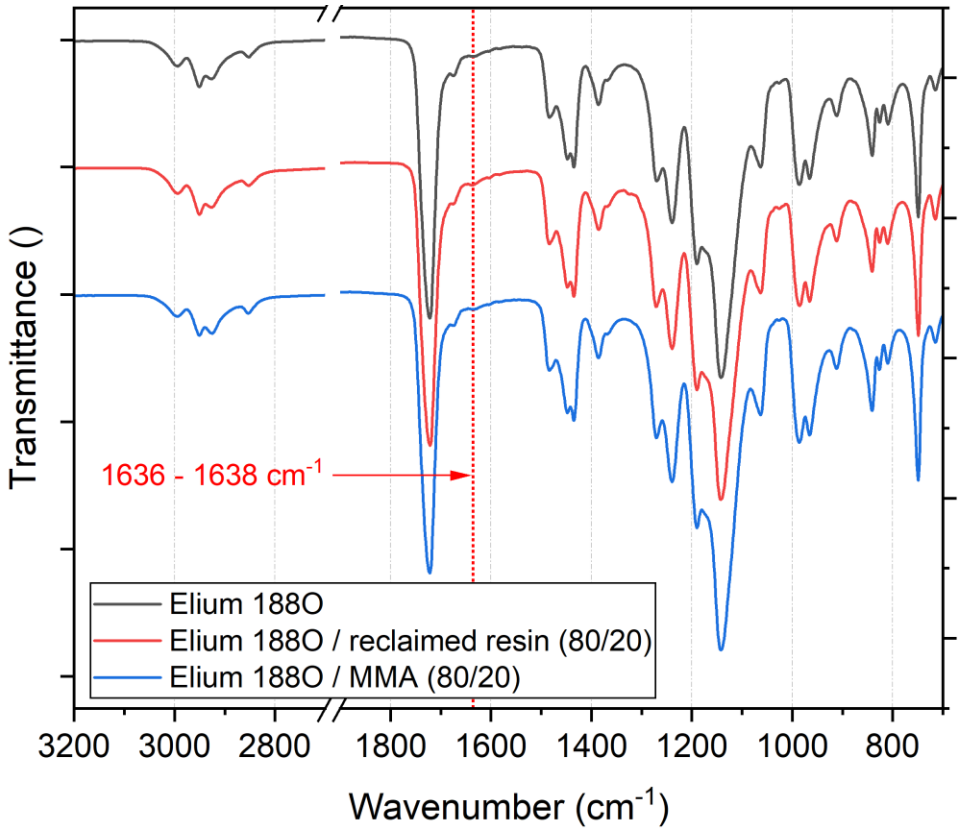

Figure 27: FT-IR spectra of polymerized Elium 188O samples.

5.3 Differential scanning calorimetry

The thermal behavior of the polymerized Elium 188O samples was analyzed using different scanning calorimetry (DSC). Measurements were performed on DSC 214 Polyma (Erich NETZSCH GmbH & Co. Holding KG) in 25 µL aluminum crucibles under N_2 (gas flow rate of 40 mL/min). The sample mass was between 13 and 15 mg. Heat flow was recorded in the temperature range between 20 and 180 °C with a heating rate of 20 K/min. The glass transition temperature (T_g) was evaluated using the mid-point temperature. Each sample was measured two times.

In Figure 28 representative DSC curves of the polymerized Elium 188O samples are shown. The average T_g values are listed in Table 11 and were between 75.8 and 97.5 °C. No significant difference between the T_g of the 100% Elium 1880 sample and the sample with 20% MMA was observed. This was expected, since the main component of Elium 1880O is MMA (>50%). In contrast adding 20% reclaimed resin resulted in an approximately 20 °C lower T_g. Thus, the other

components in the reclaimed resin significantly affected the thermal properties although only a small amount of reclaimed resin was added. This is related to inhibition of the polymerization reaction by the by-products in the reclaimed resin which results in a lower average molecular weight [18]. Consequently, also the T_g decreases.

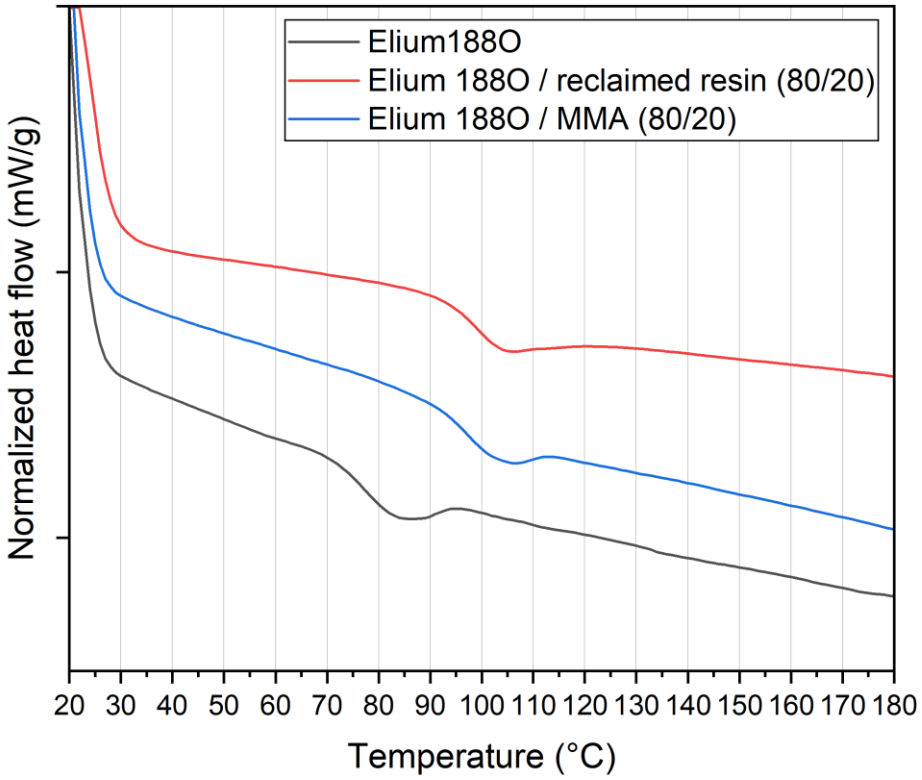

Figure 28: Representative DSC curves of polymerized Elium 188O samples with 20 K/min.

5.4 Dynamic mechanical analysis

The thermo-mechanical properties of the polymerized Elium 188O plates were determined by dynamic mechanical analysis (DMA). Measurements were performed on a DMA861^e in tensile mode with a gauge length of 19.5 mm. The sinusoidal amplitude with a frequency of 1 Hz was defined by a maximum force amplitude of 0.2 N and a maximum displacement amplitude of 20 µm. Offset control was in auto mode with 150%. The samples were characterized in the temperature range between 26 and 160 °C with a heating rate of 2 K/min. The T_g was evaluated by determining the peak temperature of loss modulus E'' and loss factor tan(δ). Cuboid shape samples with 30 x 5 x 1 mm were cut out of the plates using a water-cooled slot grinder. In order

to avoid an effect of possible water uptake on the thermo-mechanical properties, samples were dried at 50 °C for 2 h. Each formulation was measured two times.

In Figure 29 representative plots of storage modulus *E'* and tan(δ) as a function of temperature are shown. Resulting average values of determined T_g and E' at 30 °C are listed in Table 5. Evaluation of the T_g resulted in values between 59.4 and 77.6 °C by using the peak temperature of E'' and in values between 72.6 and 91.5 °C by using the peak temperature of tan(*δ*). Values for E' were between 2324 and 2989 MPa at 30 °C. By adding 20% MMA the T_g increased by 1.1 - 1.8 °C compared to the 100% Elium 188O sample. In contrast, the addition of 20% reclaimed resin decreased the T_g by 17.1 °C. This correlates with the findings from the DSC measurements. Similar results were found for E'. No significant difference for E' at 30 °C between the 100% Elium 1880 sample and the sample with 20% MMA was observed. In contrast, addition of 20% reclaimed resin decreased the modulus by 22%. This can be again correlated to a lower average molecular weight due to inhibition of the polymerization by the by-products in the reclaimed resin. Thus, in order to sustain thermal and mechanical properties the reclaimed resin must be purified and processed into a new resin.

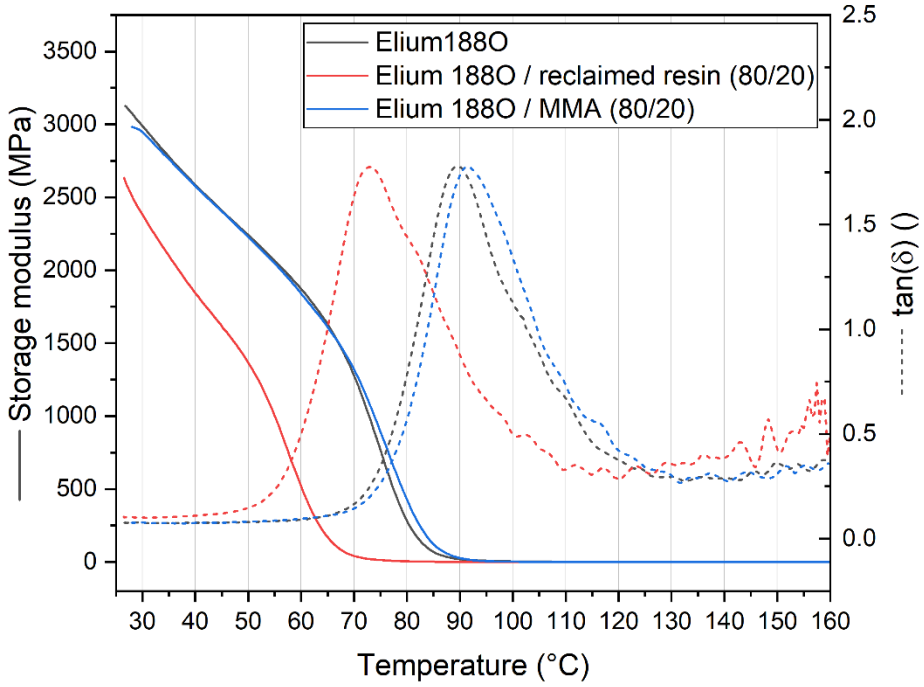

Figure 29: Representative plots of storage modulus and tan(δ) as a function of temperature of polymerized Elium 188O samples determined by DMA.

Table 11: Glass transition temperature (T_g) of the polymerized Elium 188O samples determined by DSC and DMA along with the storage modulus (E') at 30 °C.

Material	**$T_{g,mid}$ (DSC) (°C)**	**T_g (E''$_{max}$) (°C)**	**T_g (tan(δ)$_{max}$) (°C)**	**E'(30 °C) (MPa)**
Elium 188O	96.1 ± 1.1	76.5 ± 0.4	89.7 ± 0.1	2973 ± 16
Elium 188O / reclaimed resin (80/20)	75.8 ± 1.5	59.4 ± 0.2	72.6 ± 0.1	2324 ± 57
Elium 188O / MMA (80/20)	97.5 ± 1.9	77.6 ± 0.4	91.5 ± 0.1	2989 ± 42

6 Summary, conclusion and outlook

The feasibility of reclaiming monomer (MMA) from the depolymerization of Elium 188O was demonstrated by using unreinforced Elium 188O and Elium 188O reinforced with TuFF material. The small-scale depolymerization setup and the depolymerization process were systematically optimized. Depending on the initial Elium 188O mass, up to 81% of the initial Elium 188O weight was reclaimed by distillation. Mass losses were attributed to residual resin on the walls of the overall setup and to the evaporation of MMA. Overall, with a higher initial Elium 188O mass the relative mass losses decreased. Even though the carbon fibers are usually the most interesting part for recycling, the work also revealed the importance of the recycling of resin component in general. Although there is only a small amount of Elium 188O in the composite, much more Elium 188O needs to be prepared for the manufacturing process resulting in lots of waste. By collecting the excess Elium 188O for recycling, less waste is generated and the efficiency of the depolymerization process can be improved.

With FT-IR spectra the presence of MMA in the reclaimed resin was confirmed. Additionally, FT-IR measurements indicated the presence of alcohols, anhydrides, different esters, ketones or aldehydes in the reclaimed resin. The amount of MMA in the reclaimed resin was quantified using GC-FID and was between 58 and 88%. By applying a stepped depolymerization temperature (1 h at 350 °C followed by 3 h at 400 °C) and an optimized gas flow, the highest MMA content was achieved.

The reclaimed carbon fibers were not dispersible and the fibers mass was 3 - 5% higher compared to the initial fiber weight. This was mainly attributed to the formation of char but also to some residual resin on the fibers. However, with an optimized depolymerization process the amount of residue was reduced. Isopropanol and THF partially removed some particles from the fiber surfaces, but did not improve the dispersibility due to the residual resin. Furthermore, thermal post processing at 450 °C under N_2 atmosphere did also not sufficiently clean the fibers. By applying an additional oxidation step under air for 25 min at 450 °C, the fibers were fully dispersible which is crucial for the production of new TuFF feedstocks.

Besides, the effect of the addition of reclaimed crude resin (MMA content of 77%) to Elium 188O on the thermo-mechanic properties was investigated. The addition of 20% reclaimed resin lowered the T_g by 17 °C and the storage modulus E' at 30 °C by 20%. Thus, the purification and processing of the reclaimed resin is required in order to sustain thermal and mechanical properties.

Overall, the closed-loop recycling of CFRP is still a challenging topic. There is a lot of potential in achieving high quality recycled products (high purity of monomer and cleanness of fibers) by optimizing the depolymerization process. Most important parameters were found to be the applied temperature, time, gas flow, and positioning of the composite during depolymerization. Nevertheless, post processing of the reclaimed monomer is necessary which requires additional energy and the addition of petroleum-based materials. Also, obtaining recycled fibers suitable for the production of new TuFF feedstocks currently requires oxidation, which can lead to a reduced mechanical performance in the final composite.

Within this study an optimized depolymerization setup was developed, providing a basis for future research. This might include the investigation of the effect of the gas flow rate or different depolymerization temperatures on the fiber quality and the MMA content in the reclaimed resin. Furthermore, in the future additional ways to clean reclaimed carbon fibers should be explored such as ozone treatment at low temperatures.

7 Acknowledgment

First, I want to thank the Austrian Marshall Plan Foundation which provided the scholarship to make this work possible. Further, I am very grateful to the Center for Composite Materials and my supervisor Dr. Joe Deitzel who offered me this great opportunity as a visiting scholar and provided me valuable scientific input during my stay. I also would like to thank my Ph.D. supervisor Dr. Katharina Resch-Fauster for encouraging me to gain experience abroad and for the support. Many thanks also to my colleagues and new friends at the Center for Composite Materials who helped me during my stay.

This material is based upon work supported by the U.S. Department of Energy's Office of Energy Efficiency and Renewable Energy (EERE) under the Advanced Manufacturing Office Award Number DE-EE0009303.

8 References

[1] G. W. Ehrenstein, *Polymer-Werkstoffe*: *Struktur - Eigenschaften - Anwendung*, Hanser, München, 2011.

[2] J. A. Butenegro, M. Bahrami, J. Abenojar et al., “Recent Progress in Carbon Fiber Reinforced Polymers Recycling: A Review of Recycling Methods and Reuse of Carbon Fibers,” *Materials (Basel, Switzerland)*, vol. 14, no. 21, 2021.

[3] “Composites Market Size, Share & Trends Analysis Report By Product (Carbon, Glass), By Manufacturing Process (Layup, Filament, RTM), By End Use, By Region, And Segment Forecasts, 2021 - 2028,” https://www.grandviewresearch.com/industry-analysis/composites-market.

[4] A. E. Krauklis, C. W. Karl, A. I. Gagani et al., “Composite Material Recycling Technology—State-of-the-Art and Sustainable Development for the 2020s,” *Journal of Composites Science*, vol. 5, no. 1, p. 28, 2021.

[5] WindEurope, Cefic, and EuCIA, “Accelerating Wind Turbine Blade Circularity,” 9/1/2022, https://windeurope.org/wp-content/uploads/files/about-wind/reports/WindEurope-Accelerating-wind-turbine-blade-circularity.pdf.

[6] C. V. Amaechi, C. O. Agbomerie, E. O. Orok et al., “Economic Aspects of Fiber Reinforced Polymer Composite Recycling,” in *Encyclopedia of Renewable and Sustainable Materials*, pp. 377–397, Elsevier, 2020.

[7] R. Bernatas, S. Dagreou, A. Despax-Ferreres et al., “Recycling of fiber reinforced composites with a focus on thermoplastic composites,” *Cleaner Engineering and Technology*, vol. 5, p. 100272, 2021.

[8] A. Torres, “Recycling by pyrolysis of thermoset composites: characteristics of the liquid and gaseous fuels obtained,” *Fuel*, vol. 79, no. 8, pp. 897–902, 2000.

[9] O. Dogu, M. Pelucchi, R. van de Vijver et al., “The chemistry of chemical recycling of solid plastic waste via pyrolysis and gasification: State-of-the-art, challenges, and future directions,” *Progress in Energy and Combustion Science*, vol. 84, p. 100901, 2021.

[10] H. Bel Haj Frej, R. Léger, D. Perrin et al., “Recovery and reuse of carbon fibre and acrylic resin from thermoplastic composites used in marine application,” *Resources, Conservation and Recycling*, vol. 173, p. 105705, 2021.

[11] Center for Composite Materials, “Tailored universal Feedstock for Forming (TuFF),” https://www.ccm.udel.edu/research/program-highlights/tuff/.

[12] R. Emmerich, *Demonstration of Recycling of Carbon Fiber Reinforced Compo-sites using TuFF Process and Arkema Elium 188 Resin,* Master`s thesis, March 2022.

[13] A. Bahadur, S. Iqbal, H. O. Alsaab et al., “Thermal degradation study of polymethylmethacrylate with AlI3 nanoadditive,” *Microscopy research and technique*, vol. 85, no. 4, pp. 1494–1501, 2022.

[14] A. K. Nikolaidis and D. S. Achilias, “Thermal Degradation Kinetics and Viscoelastic Behavior of Poly(Methyl Methacrylate)/Organomodified Montmorillonite Nanocomposites Prepared via In Situ Bulk Radical Polymerization,” *Polymers*, vol. 10, no. 5, 2018.

[15] G. Socrates, *Infrared and Raman characteristic group frequencies*: *Tables and charts*, John Wiley & Sons LTD, Chichester [etc.], 2015.

[16] J. A. Onwudili, N. Insura, and P. T. Williams, “Autoclave pyrolysis of carbon reinforced composite plastic waste for carbon fibre and chemicals recovery,” *Journal of the Energy Institute*, vol. 86, no. 4, pp. 227–232, 2013.

[17] L. O. Meyer, K. Schulte, and E. Grove-Nielsen, “CFRP-Recycling Following a Pyrolysis Route: Process Optimization and Potentials,” *Journal of Composite Materials*, vol. 43, no. 9, pp. 1121–1132, 2009.

[18] C. B. Godiya, S. Gabrielli, S. Materazzi et al., “Depolymerization of waste poly(methyl methacrylate) scraps and purification of depolymerized products,” *Journal of environmental management*, vol. 231, pp. 1012–1020, 2019.